



André Miguel Antunes Opinião

Bachelor of Science in Micro and Nanotechnologies Engineering

Self-powered paper: Challenge to clean and green energy.

Dissertation submitted in partial fulfillment of the requirements for the degree of
Masters in Micro and Nanotechnologies Engineering

Adviser: Dr. Suman Nandy, Research Investigator, CENIMAT – i3N

Co-Adviser: Prof. Luís Miguel Nunes Pereira, Associate Professor, DCM, FCT-UNL

Examination committee:

Chairperson: Prof. Rodrigo Ferrão de Paiva Martins, Full Professor, DCM, FCT-UNL

Rapporteur: Prof. Joana Dória Vaz Pinto, Invited Assistant Professor, DCM, FCT-UNL

Member: Dr. Suman Nandy, Research Investigator, CENIMAT – i3N

December 2020



FACULDADE DE
CIÊNCIAS E TECNOLOGIA
UNIVERSIDADE NOVA DE LISBOA

Self-powered paper: Challenge to clean and green energy.

Copyright © André Miguel Antunes Opinião, Faculty of Sciences and Technology, NOVA University of Lisbon

The Faculty of Sciences and Technology and the NOVA University of Lisbon have the right, perpetual and without geographical boundaries, to file and publish this dissertation through printed copies reproduced on paper or on digital form, or by any other means known or that may be invented, and to disseminate through scientific repositories and admit its copying and distribution for non-commercial, educational or research purposes, as long as credit is given to the author and editor.

Podem tirar-me muitas coisas,
mas nunca me irão tirar a Opinião

Acknowledgements

Embora esta tese de mestrado tenha sido um trabalho individual, nunca seria possível a sua conclusão sem o apoio de certas pessoas que sempre me encorajaram durante esta fase.

Em primeiro lugar agradeço ao professor Rodrigo Martins e à professora Elvira Fortunato pela criação deste grande curso de Engenharia de Micro e Nanotecnologias e pela oportunidade de trabalhar nos centros de excelência que são o CENIMAT e o CEMOP.

I would like to express my sincere gratitude to my advisers Suman and Sumita for showing me that there no language barriers when we are talking about science. Thank you for all your hard work and support and for always being available for everything. Thank you for fighting for a greener world and for motivating us to follow your steps.

Também quero agradecer ao professor Luís Pereira por me ter dado a oportunidade de trabalhar neste projeto e por também se ter mostrado sempre disponível ao longo deste tempo.

Queria lembrar com carinho os momentos que eu e os Guilhermes (Ferreira e Coelho) entrávamos no laboratório de caracterização elétrica e os outros presentes já sabiam para o que vínhamos.

Um grande obrigado aos meus pais e ao meu irmão por me terem apoiado sempre ao longo de toda a minha vida e nunca desistirem de mim. Obrigado aos meus avós e a toda a minha família.

Obrigado à Alexandra Montes por me ter aturado este tempo todo e por me ter sempre apoiado.

Por fim, quero agradecer a todos os meus amigos do Fundão que já venho a aturar há muitos anos. E aqueles que fui criando ao longo do meu percurso académico. Sem vocês isto não teria sido a mesma coisa! Um especial obrigado à malta da residência. Nem sempre foi fácil viver com vocês, mas uma pessoa lá sobreviveu!

Abstract

In today's world, finding sustainable ways to obtain energy has become a critical issue in energy generation. As a result, research efforts in the sustainable energy have consistently focused on the generation of energy from environmentally friendly sources and reducing the use of raw and toxic materials. This thesis takes into account two very important premises: clean energy harvesting and zero e-waste. The idea behind this device is based on the mechano-responsive charge-transfer mechanism and energy-transfer process in π -conjugated polymer at the PPy/cellulose composite - electrode interface layer. When a physical deformation occurs on the surface of the polymer by a mechanical force, the charge transfer mechanism occurs and consequently the translocation of the charge carriers between the polymer and electrode. For the fabrication of the device was used an Active Layer (AL) of PPy/cellulose composite tapped to a Charge Collector Layer (CCL). It can be made from a paper-based electrode or directly created on the AL. Silver and pencil graphite were the materials chosen for the electrode. 0.91 Wm^{-2} and 23.5 mA m^{-2} current density and power density, respectively, were obtained for the both developed devices. This technology could be very promising in the area of security systems with the use of code bars and can also be used for energy harvesting system.

Keywords: Paper Electronics, Clean Energy, Mechano-stimulli, Charge Transfer, Zero e-waste, Polypyrrole/Cellulose system.

Resumo

No mundo atual, encontrar alternativas sustentáveis para se obter energia tem se tornado um problema crítico na produção de energia. Como resultado, os esforços na investigação em obtenção de energias sustentáveis estão focados na produção de energia verdes e na redução do uso de matérias-primas e tóxicas. Esta tese de mestrado tem em conta duas premissas muito importantes: recolha de energia limpa e zero lixo eletrónico. A ideia que tem por base este dispositivo é baseada na resposta de um estímulo mecânico que produz um mecanismo de transferência de cargas e no processo de transferência de energia num polímero π -conjugado no compósito de celulose/PPy – interface do eletrodo. Quando ocorre uma deformação física na superfície do polímero devido a atuação de uma força mecânica, ocorre o mecanismo de transferência de cargas e, conseqüentemente, a translocação dos portadores de carga entre o polímero e o eletrodo. Para a fabricação do dispositivo foi utilizada uma Camada Ativa composta por PPy/celulose em contacto direto com uma Camada Coletora de Carga. Esta camada pode ser feita separadamente em papel ou criada diretamente na Camada Ativa. Os materiais escolhidos para serem usados como eletrodo foram: prata e lápis grafite. Foram obtidas densidade de corrente máxima e densidade de potencia máxima de 0.91 Wm^{-2} and 23.5 mA m^{-2} , respetivamente. Esta tecnologia pode ser muito promissora na área de sistemas de segurança com a utilização de códigos de barras e também pode ser usada para sistemas de recolha de energia.

Palavras-chave: Eletrónica de Papel, Energia Limpa, Transferência de Carga Mecanicamente Estimulada, Baixo Resíduo Eletrónico, Sistema Polipirrol/Celulose

Contents

Acknowledgements.....	i
Abstract.....	ii
Resumo.....	iii
Contents	iv
List of Figures.....	vi
List of Tables	viii
List of Abbreviations	ix
List of Symbols	x
Motivation and Objectives	1
1. Introduction	2
1.2 Circular Economy: Paper is an Option.....	2
1.3 Conjugated Polymers.....	3
1.4 Charge Transfer Mechanism	4
1.5 Mechanical Energy Harvesting.....	5
1.6 Pencil Graphite Electrode	6
2. Materials and Methods	7
2.1 Main Reagents	7
2.2 Pixelating the Paper.....	7
2.3 Functionalization of paper with polypyrrole (FPP)	7
2.4 Fabrication of self-powered paper	8
2.5 Characterization Techniques.....	8
3. Results and Discussion	9
3.1 Chemical and Morphological Analyses	9
3.2 Electrical Analyses.....	11
3.3 Self-powered paper: Real-Field Applications	16
3.4 Green device: A proof of biodegradability	20
4. Conclusions and Future Perspectives	21

5. References.....	23
Annexes	25
<i>Annex 1. – Chemical and Morphology Analyses.....</i>	<i>25</i>
<i>Annex 2. – Electrical Analyses.....</i>	<i>27</i>
<i>Annex 3. – Self-powered paper Real- Field Application</i>	<i>28</i>
<i>Annex 4. – Self-powered PDMS device.....</i>	<i>29</i>

List of Figures

Figure M.1: Sustainable development goals defined by U.N. for the "2030 Agenda for Sustainable Development". The highlighted objectives are those that we will directly or indirectly contribute to. ...	1
Figure 1.1: E-waste produced by each continent in 2019	2
Figure 1.2: The new concept of circular economy. Paper is one of the major choices.	3
Figure 1.3: Schematic illustration of charge transfer mechanism: (a) no stress applied, the charge transfer mechanism does not occur; (b) under stress condition: charge density increase, and the charge carriers begin translocation to the electrode in the pressurized area; (c) mechanical stress relief: the pressure is released resulting in a localized electron scarcity which will be attenuated by charges from neighboring networks.	5
Figure 2.1: Image of wax-printed pixelates paper substrate.....	7
Figure 2.2: (a) Schematic of the functionalization of paper via in-situ polymerization process using the drop-cast technique. Image of PPy functionalized paper of (b) front side and (c) back side respectively.....	8
Figure 3.1 : FESEM images of the FPP, from (a) the front side (drop-cast side) and (b) the back side. Inset shows the high-resolution microstructure of polypyrrole.....	10
Figure 3.2: Raman Spectra of the frontside and backside of FPP and raw paper.....	11
Figure 3.3: (a) Drawing the graphite pencil electrode directly on the FPP; (b), (c) Lateral resistance of 6B and 8B pencil electrode; (d),(e) Mechano-responsive output voltage and current, respectively, of 6B electrode device; (f),(g) Mechano-responsive output voltage and current, respectively, of 8B electrode device.	12
Figure 3.4 - Figure 10: Schematic design of three different architectures of paper-based energy harvesting devices and their real images.	13
Figure 3.5: (a),(b) Mechano-responsive output voltage and current, respectively, of device with separation of electrode; (c)(d) Mechano-responsive output voltage and current, respectively, of device without separation of electrode.	14
Figure 3.6: Results obtained for the current density and power density curves and schematic of rectifier circuit: (a) Paper-based device with separated silver electrode; (b) Paper-based device without separated silver electrode; (c) (b) Paper-based device without.	15
Figure 3.7: Schematic of frontside and backside of a Tag device used for security systems. Consisting of broader lines and thinner lines and without separating the electrode with the AL.	16
Figure 3.8: Swipe test that is performed in less than one second with a finger to slide over the tag: (a), (b), (c) The results obtains are the V_{oc} . It is possible to observe that the broader lines have an output voltage of about 3V and for the thinner lines 2V. The voltage can be classified in a binary system, with 1 being the highest and 0 the lowest.	17
Figure 3.9: An illustration of future application of self-powered electronic tag, which can be embedded in personal ID card or packaging. The particular arrays of device will generate particular electrical signal, which can be converted as binary code and transmitted through wireless and communicate with the security system such as “Door Open”, or “Product Authentication”.....	18
Figure 3.10: Schematic of "RGB device": Showing three touch-interactive energy harvester devices connected to an Arduino. When one or more devices are pressed, and the Arduino will receive this	

input and will return the associated color or colors. This output will be sent via the ESP32 microcontroller, which has Wi-Fi. A computer connected to a Wi-Fi network will receive the information and show the color. In this particular case, the example for the red color is shown.	19
Figure 3.11: Snap shots of the device burning process. Raman spectroscopy analysis of black residuals that has been achieved after burning the device.....	20
Figure A.1: FESEM image of raw Whatman Chromatography Paper.....	25
Figure A.2: Humidity sensor setup.....	26
Figure A.3: a) I-V curves of the humidity sensor at different relative humidity. b) Graphic of device resistance at different relative humidity.	26
Figure A.4: Snapshot of the connections of each line of Tag device with oscilloscope.	27
Figure A.5: Snapshot of 53 LEDs lighting up during performance tests.	27
Figure A.6: RGB Color Codes Chart	28
Figure A.7: a) The PDMS device before Kapton peeling off, b) PDMS devices without and with Polypyrrole after peeling off, respectively.	29

List of Tables

Table 1: Electrical characterization results for the paper-based devices with different electrode material.....	15
--	----

List of Abbreviations

AC – Alternating Current

AL – Active Layer

APS – Ammonium Persulfate

CCL – Charge Collector Layer

e-waste – Electronic Waste

EDS – Energy Dispersive Spectroscopy

EFM – Electrostatic Force Microscopy

FESEM – Field Emission Scanning Electron Microscopy

FCP – Functionalized Chromatography Paper

FPP – Functionalization of paper with PPy

MMt – Million Metric tons

PANI – Polyaniline

PPy – Polypyrrole

TENG – Triboelectric Nanogenerator

U.N. – United Nations

WCP – Whatman Chromatography Paper

List of Symbols

I – Current

e – Elementary charge

I_{max} – Maximum current density

P_{max} – Maximum power density

V_{oc} – Open circuit voltage

P – Power

R – Resistance

I_{sc} – Short circuit current

Motivation and Objectives

There is only one planet Earth, yet by 2050, the world will be consuming as if there were three. ^[1]

The world of the 21st century is witnessing different global crises. Among them, some of the most worrying crises are social, political, economic and environmental. In the environmental crisis the biggest challenges are climate change and global warming. One of the small steps that can be taken in this work for this struggle are the contribution to reduce e-waste, the reduction of the dependence on raw materials and the production of clean energy.

This work meets the guidelines given by the 2030 Agenda for Sustainable Development and Green Deal. However, a global effort is needed for change to happen.

Paper has gained an increasing importance in the scientific area in recent times and especially in the electronics area. It is being widely used as a substrate due to simple manufacturing, easy recyclability, low-cost and lightweight. There are many works published in this area, from supercapacitors, microfluidic devices to smart sensors. However, mechanical harvesting technology has not been widely studied.

The development of a paper-based mechano-responsive energy harvester device, that is low-cost and can be 100% recyclable or that produces the minimal amount of waste, is the main goal to achieve in this thesis. In our device the paper was functionalized with a conjugated polymer, in this case Polypyrrole (PPy). The polymerization forms a cellulose/PPy composite that promises a good potential in energy harvesting and it was also used in some devices with pencil graphite electrodes.



Figure M.1: Sustainable development goals defined by U.N. for the "2030 Agenda for Sustainable Development". The highlighted objectives are those that we will directly or indirectly contribute to.

COVID-19 did not stop climate change nor our fight against it. This thesis is our contribution in the fight against the climate change (SDG 13) and respecting the issue of resources limitation and the environmental pollution (Green Deal). The technology present in our device allows access to green and portable energy (SDG 7). These technological advances can be scaled to the industrial level (SDG 9), being able to generate new qualified jobs and potentiate the economic growth (SDG 8) and also will contribute for smart and sustainable cities and communities (SDG 11).

1. Introduction

1.1 e-Waste: The greatest threatening for Earth

With the world's growing population, where the economic prosperity reaches more people, consumer market is spreading rapidly. Among all the consumers products, technological development is growing quickly because of its low-price cost while they make the consumers life smarter. But, with dropping prices, electronic products are also leading to shorter product lifespans which is creating the greatest ever problem of electronic waste or e-waste. This results in one of the major problems in current world and a threat to our planet due to the toxic materials that are present in most of the electronics components, which is a serious environmental risk to our soil, water, air and wildlife.

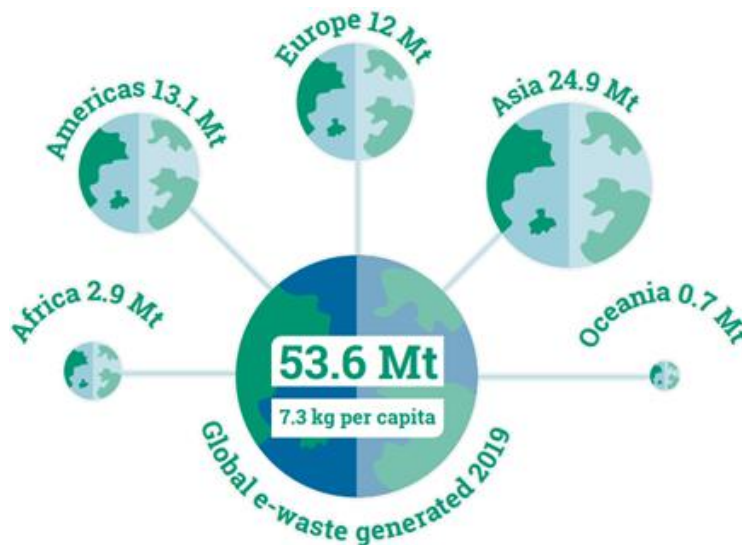


Figure 1.1: E-waste produced by each continent in 2019

According to the U.N. in 2016, the value of expected for 2021 was about 52.2 million metric tons (MMt).^[2] Surprisingly, in 2019, the world already surpassed that amount generating 53.6 MMt e-waste, and it is projected to grow to 74.7 MMt by 2030 which is almost the double in just 16 years.^[3] In 2019, only 9.3 MMt was recycled in the whole world that represents just 17.4% of all the e-waste generated; while the rest 82.6% had an uncertain destiny adding to that a considerable amount of e-waste is exported illegally to low-income countries.

Therefore, it is extremely important that we invest more on sustainable technologies, study efficient ways to recycle e-waste and educate people to raise awareness to the dangers of this kind of waste. Taking this into account it is essential that the scientific community be the first to take the initiative to use environmentally friendly materials and use zero e-waste policies and, at the same time, continue to seek new strategies against global warming and the energy crisis.

1.2 Circular Economy: Paper is an Option

Key materials for industrial societies and applications require natural resources from our Earth. But in traditional economy these needs are satisfied only by extracting and processing resources and trading them for further manufacturing. The usage of global resource could be doubled between 2010 and 2030.

However, the major of those resources is not reused or recycled and ending up as waste often burned or landfilled. This results a tremendous economic problem and a supply risk.

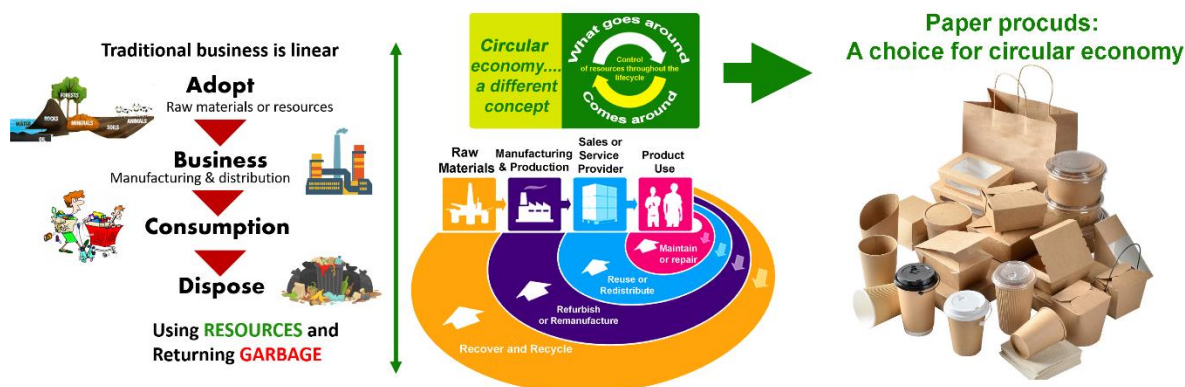


Figure 1.2: The new concept of circular economy. Paper is one of the major choices.

The concept of circular economy aims to overcome this linear economic concept of “Take-Make-Dispose” and creating a new concept of “Reduce-Reuse-Recycle. Circular economy promises economic and social prosperity by limiting the impacts of the current economic structure, reaching from social inequality to depletion of natural resources and environmental pollution. The transition to the circular economy is inevitable. This new economic system will be an indispensable part of the new European Union industrial strategy. This system will allow to save up to 600 billion euros and will create 580 000 jobs only in the EU. It will allow economic growth while permitting the reduction of carbon emissions to 450 million tonnes by 2030.^[4]

Using biocompatible materials as more as possible and adopting circular economy will help us to overcome this situation. In this aspect, paper’s role in circular economy is very important. Paper or cellulose originates from living elements, and is 100% biodegradable, lightweight and abundant, and can be also recycled more than any other solid waste. Packaging industries are one of the biggest commodities that not only requires to protect the manufacturing product but also provide the product information. On the other side, last few years cellulose or paper has been utilized in electronics. Cellulose has revealed itself as a promising substrate material for new electronic purposes, such as transistor,^[5] energy applications,^[6] microfluidic analytical devices,^[7] biosensors etc. Very recent, paper or cellulose substrate is also employed in energy harvesting system using simple graphite pencil drawn electrode. The device shows a good electrical performance with a voltage, current, and power density of 85V, 3.75 μ A, and 0,398 W m⁻² respectively.^[8] Therefore, paper or cellulose combined with electronics opens up a new door for smart packaging industries, which can reveal a ultra-new product in security systems such as electronic barcodes or tag, while promoting circular economy and green and sustainable economy in future.

1.3 Conjugated Polymers

A polymer is a material that has a long chain of molecular structures and mostly is an insulator by nature. But interestingly, conjugated polymers can be synthesized as electrically conductive through doping-dedoping processes during the polymerization process. The main reason behind these good electrical properties is π -electron bonds that enable the electrons to delocalize thus creating a good charge transfer mechanism between the molecular network.^[9] Several conjugated polymers (CPs) such as polyaniline, polypyrrole, PEDOT:PSS, P3HT have been intensively investigated. They are extremely attractive due to ease of production, excellent electrical conductivity, mechanical flexibility and a good cost effectiveness. With the emergence of this technology, different electronics applications start to appear

as supercapacitors,^[10] Polymer organic light-emitting diodes (PLED),^[11] chemical sensors,^[12] biosensors,^[13] biomedical applications^{[14]–[16]} and Lithium ion batteries.^[17]

Among all the CPs, Polypyrrole (PPy)^[18] and Polyaniline (PANI)^[19] are used extensively in the field of energy harvesting by different research groups. These materials are widely used as a electrode material for storage devices, supercapacitors, and batteries.^{[20], [21]} Interestingly, very recent, this conjugate materials are also investigated as mechano-responsive energy harvester application, where materials itself takes part as an active layer.^[22] It shows that, with the presence of mechanical stress-release condition, these conjugated polymers initiate the charge transportation mechanism, that is able to generate electrical energy.

It would be further interesting to combine these CPs with cellulose substrate and employed it to energy harvesting applications. In this thesis work, we have investigated PPy/cellulose composites paper substrate for mechano-stimulus energy harvester. With the simple graphite pencil drawn electrode on the PPy/cellulose paper substrate designed ready to use device. And this takes technology a step further in the area of sustainability. Since the devices are close to zero-e-waste.

1.4 Charge Transfer Mechanism

The fundamental idea of this energy harvesting system using a PPy/cellulose composite is to study the mechano-responsive charge transfer mechanism of π -conjugated polymers at the electrode/polymer interface layer (**Figure 1.3**). When a localized mechanical stimulus is exercised on electrode/polymer interface, the result will be an increase of localized electron density that promotes a Fermi-level pinning and the charge carriers will transmute from polymer to the nearest available energy state, which is the charge collector electrode. When the stimulus is liberated, the polymer network structure will expand, thus will result in a localized electron scarcity. The surrounding region that has a much higher electron density, will balance out this electron scarcity, by hopping mechanism, allowing a new cycle of pressure.

In this thesis, it will be presented a low-cost paper-based energy harvester, responsive to a mechanical interaction. Much of the mechanical energy produced by the human body motion is dissipated, so the main aim is to get an electrical output signal from that motion. The drop-cast technique at room temperature with an ice bed was used for the functionalization of chromatography paper via in-situ polymerization.

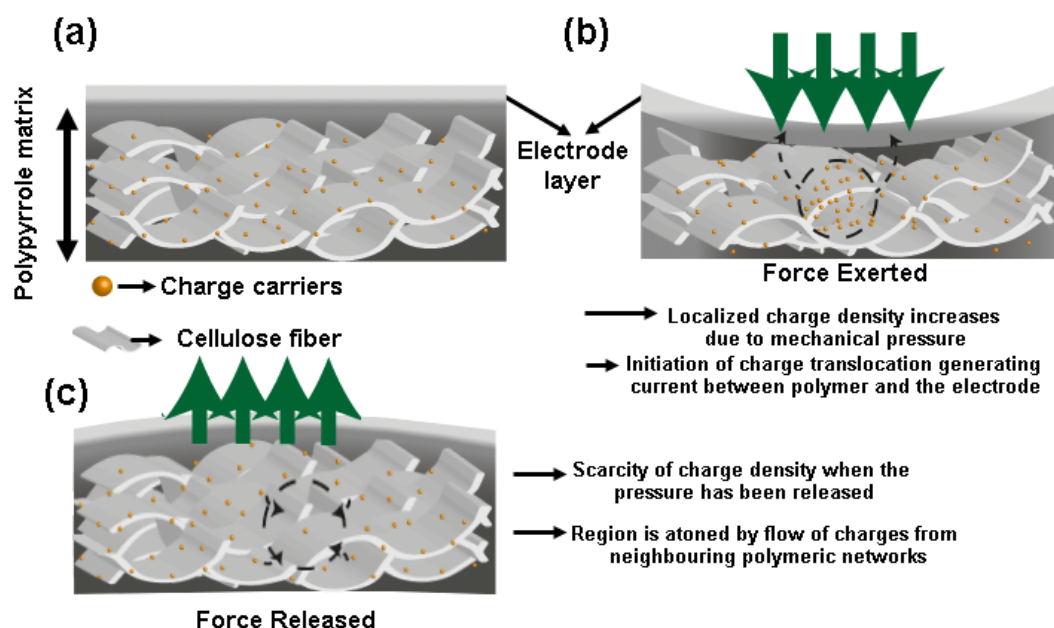


Figure 1.3: Schematic illustration of charge transfer mechanism: (a) no stress applied, the charge transfer mechanism does not occur; (b) under stress condition: charge density increase, and the charge carriers begin translocation to the electrode in the pressurized area; (c) mechanical stress relief: the pressure is released resulting in a localized electron scarcity which will be attenuated by charges from neighboring networks.

1.5 Mechanical Energy Harvesting

The growing increment in energy demand leads to a higher CO₂ emission every year. So, the need to transit from fossil fuels to sources of green energy is essential. Nowadays, we already use different types of renewable and sustainable energies like solar, wind, geothermal and Hydroelectricity, etc. There is one energy in particular that is wasted everyday by us when we walk, drive or even by nature (ocean waves, wind blowing, rain, etc.), and that is mechanical energy.^[23] That kind of energy has great potential to be harvested and transformed into electricity. This technology can be used in an energy harvesting system, but also in many more areas such as the security, sensors, tracking and identification system. Because of its, energy harvesting ability, this mechanism can also be applicable to build a Self-Powered Identification System.

Mainly, two types of materials are hugely used for mechanical energy harvesting system: (i) piezoelectric materials and (ii) triboelectric materials. Piezoelectric materials have the capability to produce charges when they are submitted to an external mechanical stimulus. They can work in two modes: direct and reverse. On the direct mode if the material is under a mechanical stress or strain it will produce charges. This implies that these elements convert mechanical energy into electrical energy. The reverse effect or the opposite effect, happens when we apply an electrical stimulus and a displacement occurs in the piezoelectrical material. When a mechanical force is applied, an electrical voltage or current is created due to the uniform distributions of positive and negative charges. So, an electrical current is created when a piezoelectrical material deforms and the charges get unbalanced.^[24] On the other side, triboelectric effect is a type of contact electrification where two materials become electrically charged when they come into contact by friction. The contact electrification is the process

of electron transfer based on the difference in work function of different materials. When two materials come in contact the chemical bond formed between the two surfaces allow the charge transfer and balanced their electrochemical potential.^[25] The charge transfer mechanism is more closely related to the triboelectric effect. The piezoelectric system works on the polarity of inter charges instead of localized charges which is the principal that defines the charge transfer mechanism.^[26]

Piezoelectric generators have been explored in different type of fields. Such as medical implants like pacemakers, wireless sensor networks, monitoring system for bridges, buildings and tire pressure. For energy harvesting system the piezoelectric generators are used on wearable technology like shoes or clothes using mechanical energy dissipated by human body.^[27]

The triboelectric nanogenerators (TENGs) are also gaining a prominent place within the scientific community. There are four modes of TENGs, in which they can operate: Vertical contact-separation, contact sliding, single-electrode and freestanding triboelectric-layer. There already exists some TENGs based on paper. In single-electrode mode, the electrode is in contact with the active layer. Some researchers have reported on single-electrode devices where the maximum power density can reach up to 8.44 mW m^{-2} ^[26] and there is also some paper based TENG in contact-separation operating mode with a high output voltage and power density of 60 V and 0.83 W m^{-2} .^[28]

In this section, conjugated polymers are the uncommon and innovative choice that has been investigated for mechanical energy harvesting applications due to their electrical conductivity and flexibility.

1.6 Pencil Graphite Electrode

Carbon is very commonly used as an electrode in electrical devices for their intrinsic properties. The reason for the high electrical conductivity and mechanical robustness is its graphitic structure. Carbon is very abundant in our planet and cheap when we compare with other conductive materials that can be used as electrodes. One of the forms of carbon is graphite. Graphite is considered as a semi-metal that has both metallic and nonmetallic properties, being very useful as an electrode material. The pencil graphite leads are composite materials containing graphite (~65%), clay (~30%), and a binder (wax, resins, or high polymer). ^[29]

The European Letter Scale defines that graphite pencils need to be marked with numbers that stipulate the degree of hardness or blackness from 9H to 8B (the hardest to the softest), and letters H(hardness) and B(blackness). The B-type is softer and contain more graphite, and the H-type is harder and has more clay, also exists the HB-type which contains the same amount of graphite and clay.

For our purposes it was decided to use the 6B and 8B pencils because they have the highest percentage of carbon (84% and 90%, respectively) which should result in greater conductivity.

2. Materials and Methods

The next section will present all the steps needed to the fabrication and characterization of Self-powered paper functionalized with PPy.

2.1 Main Reagents

Pyrrole monomer ($\geq 98\%$, Sigma-Aldrich), ammonium persulfate (APS; 99.99%, Sigma-Aldrich) and hydrochloric acid (HCl; $\sim 37\%$, Alfa Aesar) are the principal reagents for the polymerization via *in-situ* of Polypyrrole (PPy). Deionized water (DI) (obtained through Elix® Advantage 3 Water Purification System) was used during all the experiments and washing procedures.

2.2 Pixelating the Paper

Due to the use of the drop-casting technique, it is impossible to limit the dispersion area of the applied solution. To solve this problem, it was necessary to create a physical barrier, where wax-printed square-shaped wells (1cm^2 area each, **Figure 2.1**) in the form of an array (7×4) and a solid wax (Ref:108R00935, Black) in an office laser printer (Xerox ColorQube 8580) was used. After printing is complete, the paper must be heated to 100°C on a digital hot plate providing a flat and a constant heat rate so that the wax will melt and form a hydrophobic barrier, that retains the drop-casted solutions on a hydrophilic paper. Each pixel has a known area of $10 \times 10\text{ mm}^2$. The Paper used for all devices was a Whatman™, Chromatography Paper (WCP), Grade: 1 CHR.

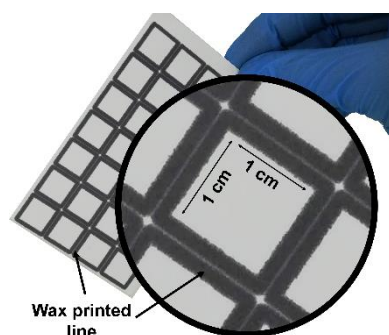


Figure 2.1: Image of wax-printed pixelates paper substrate.

2.3 Functionalization of paper with polypyrrole (FPP)

For the functionalization of paper with PPy (FPP), *in-situ* polymerization reaction has been done in each pixel area individually (**Figure 2.1**). First, it was prepared an oxidizing aqueous solution (APS solution) from the addition of 1.3g of APS to 10mL of DI water and left under stirring for 5min. After that 125 μL of HCl was added to the solution and left under stirring for about 10 min until the solution was completely homogeneous. The polymerization of Polypyrrole was done by two-step drop-casting method. The APS solution was drop-casted on top of the paper followed by drop-cast of the Pyrrole monomer, in a volume ratio of APS solution: Pyrrole monomer of 6:1. For each pixel, the amount used was 12 μL of APS solution and 2 μL of Pyrrole monomer and were previously placed in an ice bath for 30 min before the drop-casting. The reaction occurs on an ice bed and needs seconds to be completed-to observe an almost instant change in the color of the paper surface to dark blue. And then FPP was left to dry at room temperature. This FPP work as Active Layer (AL).

2.4 Fabrication of self-powered paper

After the FPP is completely dried, it is necessary to integrate with electrode, which will work as a Charge Collector Layer (CCL). The electrode was either placed directly on the surface of the functionalized paper (with physical separation) or developed on the functionalized paper surface (no physical separation). Different types of electrodes were used (graphite and silver) to study the influences of the electrodes and device structure. Due to limited space in Materials Section (2 pages), they are presented later in results and discussion section in **Figure 3.4** showing the schematic design of three difference device fabrication method and the snapshot of real devices.

Two different grades of pencil graphite: 8B (Faber-Castell, Castell 9000) and 6B (Faber-Castell, Goldfaber 1221) were used as electrodes where it was drawn over the active layer until a uniform layer was obtained. For Silver (CRSN2442 AG INK, Coated Screen Inks), electrodes were screen-printed on top of the active layer or for the external electrodes were screen-printed on another paper and for both electrodes, they were dried on a hot plate at 60°C for 15 minutes.

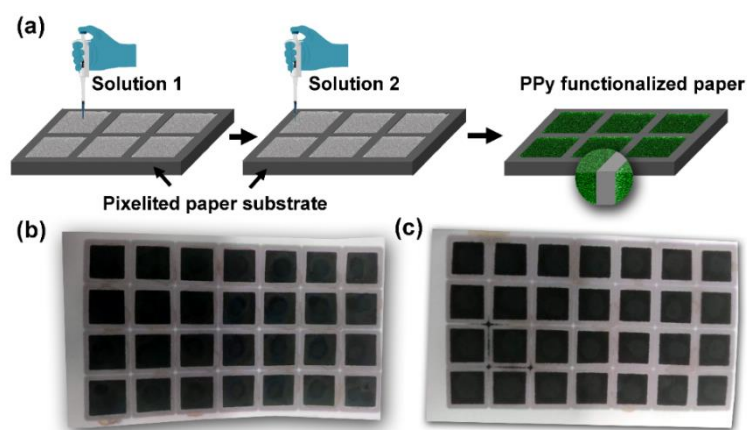


Figure 2.2: (a) Schematic of the functionalization of paper via in-situ polymerization process using the drop-cast technique. Image of PPY functionalized paper of (b) front side and (c) back side respectively.

For the fabrication of device, several layers have been integrated into one. The FPP, which correspond to the Active Layer, will be in contact with the Charge Collector Layer. The CCL consists of the screen-printed silver electrode or the pencil-drawn graphite electrode directly on top of the active paper, this is for the device without physical separation. For the device with physical separation, the CCL will consist of a separate paper-based electrode, that will be in contact with the PPY functionalized paper within device *i.e.* FPP. For the finalization of the device, it was encapsulated properly to avoid handling effects. The materials used for the encapsulation were office paper or sponge paper. All the layers were tapped together with commercial office tape. The active area used on the device of the functionalized paper was for a 2×3 matrix, each pixel with a total functionalized area of 1 cm^2 .

2.5 Characterization Techniques

The chemical structures of the samples are characterized by Raman spectroscopy (Renishaw Qontor InVia Raman microscope) using the 532 nm excitation laser line with 10% of the maximum laser power (50 mW) and 1s exposure time for each 10 accumulations. The mechano-electrical studies were performed by recurring to a digital storage oscilloscope, (Tektronix TBS 2022). Morphological analyses were performed using a field emission scanning electron microscope (FESEM-FIB, Carl Zeiss Auriga Crossbeam microscope).

3. Results and Discussion

The functionalization process requires a relatively easy preparation. The presence of the black color on both sides of the paper indicates that polymerization occurred. Therefore, we can confirm that solutions have impregnated all the paper, due to capillary effects. Both reactants penetrate the cellulose microstructure allowing the polymerization reaction to occur everywhere. The raw paper used has the property of being highly porous, which allows the diffusion through the structure of the solutions and that results in a fully functionalized paper.

The PPy production is affected by different factors, like the choice of oxidant and solvent, pyrrole/oxidant ratio and the temperature of the reaction. For our needs, it is important that PPy/Cellulose composite have a good behavior to mechanical stimulus and that it does not peel off from the surface in a short time.

There are two different phases of PPy: Neutral (undoped) and Oxidated (doped). For our work we focused on the oxidated phase because of its semiconducting nature.

The synthesis of PPy can be achieved by several processes such as oxidative chemical technique, electrochemical synthesis, microemulsion polymerization, and, micellar polymerization, etc. For our purposes we go for the oxidative chemical technique because of the simplicity of the process.

3.1 Chemical and Morphological Analyses

According to the literature survey, ferric chloride (FeCl_3) is commonly used as an initiator oxidizing agent during the polymerization of PPy. The presence of FeCl_3 influences the electrical conductivity and even on the morphological structure of the polypyrrole.^[30]

In general, the conductivity obtained through chemical processes in acidic solution, using FeCl_3 as initiator, is between $10^{-3} \text{ S cm}^{-1}$ to $10^{-2} \text{ S cm}^{-1}$. There are studies that used ammonium persulfate (APS) as an initiating agent to synthesize PPy in acidic solution and conductivities in the order of $10^{-2} \text{ S cm}^{-1}$ to $10^{-1} \text{ S cm}^{-1}$ were obtained.

There are various oxidant agents that we can use for the redox reaction initiator: Ammonium Persulfate (APS), Hydrogen peroxide, Cerium (IV) Sulfate, Potassium dichromate and Ferric chloride. The oxidation potential (E_0) is of 1.94V, 1.78V, 1.72V, 1.23V and 0.77V, respectively. It has been chosen the APS because oxidation potential is higher than the others.

When PPy is doped, π -electrons are removed from the higher level of the valence zone and at the same time a shift of the boundary π -levels to lower energies. When an electron is removed from the backbone produced a free radical and a positive charge. The formations of a polaron are equivalent to formation of a radical cation and of a bipolaron, to dication. The creation and separation of these defects cost a considerable amount of energy. This limits the number of quinoid-like rings that can link these two bound species together. The polaron and bipolaron in PPy are extended structures spread over three or four monomeric units of the chain. The separation of the positive charge on the chain in the bipolaron structure predetermines the energy of the system. The further the positive charges are apart the lower the stability of the system since it contains more rather unstable quinoid rings.^[31]

There are several surfactants that can be used for controlling the morphology and the stability of the PPy. However, this will also compromise the conductivity of PPy. These additives will affect the ordering of PPy chains grow because the hydrogen bonding between polypyrrole units promotes the chain ordering and may disturb the organization of chains and thus reduce the conductivity.^[32]

During the experimental work one surfactant CTAB was used, but the results were not as expected, and the surface stabilization did not occur as intended. So, no type of surfactants was used further.

The optimization of the cellulose/PPy composite Layer was one of the most time-consuming tasks in this thesis due to constant changes in temperature and humidity in the laboratory. Though humidity can have a major negative influence on polypyrrole. Some tests were carried out with the active layer in a humidity box in order to better understand the influence of humidity on the devices (See **Annex 1**).

The surface morphologies of the top and bottom of FPP were characterized by FESEM that is shown in **Figure 3.1** with the purpose to observe the formation of PPy/cellulose composite. It can be clearly seen that both side paper surfaces are coated with PPy indicating complete functionalization of paper. In both surfaces it is possible to observe a cauliflower-like morphology constituting of globular grains.

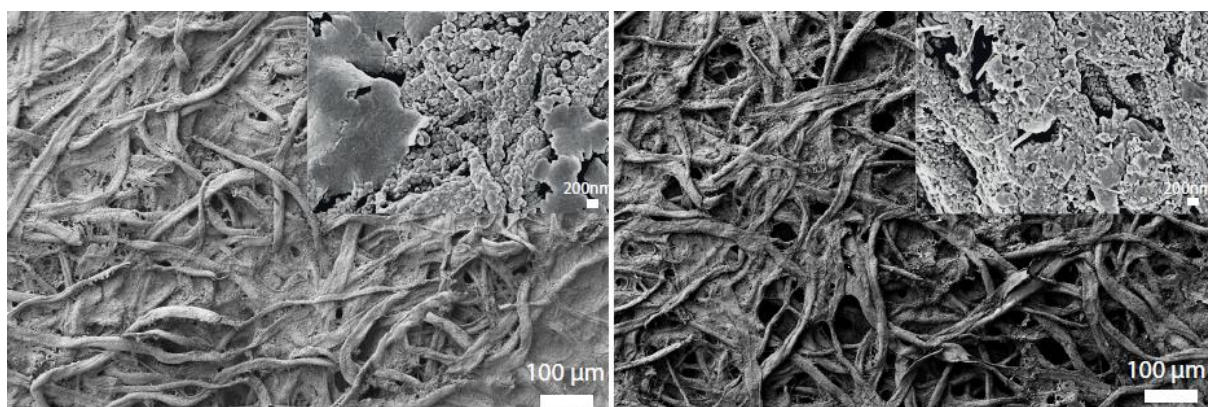


Figure 3.1 : FESEM images of the FPP, from (a) the front side (drop-cast side) and (b) the back side. Inset shows the high-resolution microstructure of polypyrrole.

The rate and agitation of polymerization depends on the various synthesis conditions such as, reaction time, temperature, pH, oxidant type, ratio of the oxidant to the monomer concentration, and solvent type that can easily change and influence the morphology and size of PPy granules. The use of surfactant/stabilizer can also affect the morphology structure of PPy but it was decided to not use it in this work.

The electrical conductivity of the produced PPy films is also affected by synthesis temperature. Polypyrrole when synthesised at a lower temperature exhibits longer conjugation length, structural order, fewer structural defects, and higher conductivity.^[33]

The Raman Spectroscopy tests were conducted to determine the chemical composition on both sides of the FPP and the raw chromatography paper (control sample) that is shown in **Figure 3.2**. Both sides of the functionalized paper have an identical Raman spectrum. The main band of PPy is located at $\sim 1579 \text{ cm}^{-1}$ that corresponds to C=C stretching vibrations in-ring and C—C inter-ring in the backbone appear from polaron and bipolaron structures. The bands 1340 cm^{-1} and 1384 cm^{-1} correspond to different vibrations of pyrrole ring which is constituted with polaron and bipolaron structure. The peak at 1052 cm^{-1} is associated to symmetric C—H bending vibrations and N—H deformation vibrations of the ring with cation-radical is caused by polaron structure in polypyrrole chain. The bands 935 cm^{-1} and 970 cm^{-1} are related to C—C vibration in bipolaron and polaron structure, respectively.^[34] The conductivity of PPy is related to the position of the band belonging to vibration C=C/C—C ($\sim 1579 \text{ cm}^{-1}$)

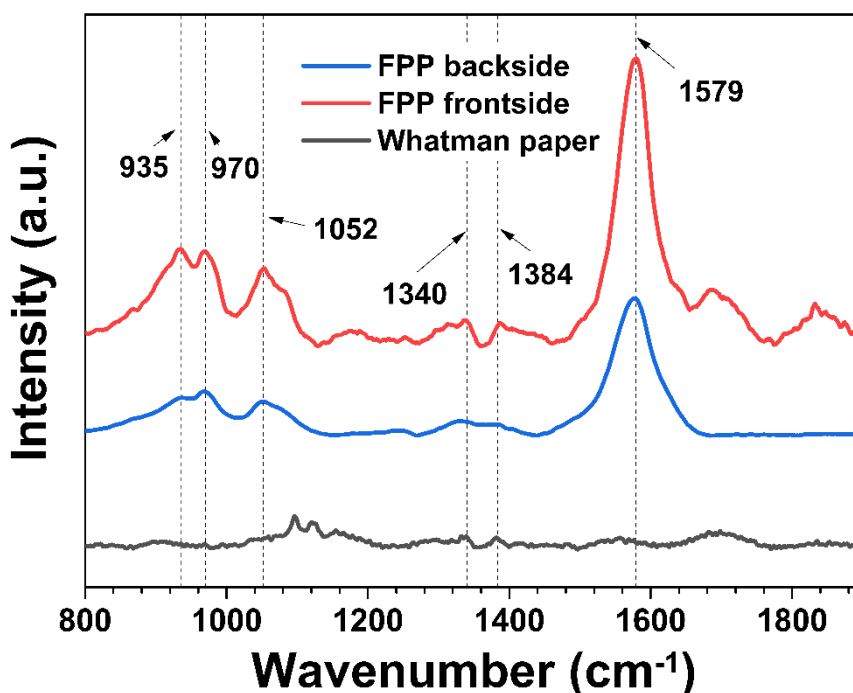


Figure 3.2: Raman Spectra of the frontside and backside of FPP and raw paper.

3.2 Electrical Analyses

After the functionalization of the paper through the polymerization of pyrrole, the first test that is performed is the measurement of the cross-section and lateral resistances of the functionalized paper. One of the major problems of FPP conductivity is the wide variation in results. For the functionalized paper, we can report lateral resistance values between $386 \, \Omega$ and $2000 \, \Omega$. And the cross-sectional resistance is around $700 \, \Omega$. PPy/cellulose composite reveals a great conductivity of $0.14 \, \text{S m}^{-1}$.

The electrical conductivity of PPy is the product of two important factors, the number of carriers and charge carrier mobility. Higher mobilities will occur with more crystalline, better oriented structure. Increasing the doping level will increase the density of charge carriers. So, the conductivity is highly dependent on the level of protonation.

Taking the zero-e-waste policy into account the devices shown above are good example for low-cost sustainable and green technology. The device allows the generation of electrical energy by a mechanical stimulus through the charge transfer mechanism in the PPy/cellulose composite system as mentioned earlier. The device was prepared with simple procedure where graphite pencil was used to draw electrode layer directly on the FPP. Therefore, both the active layer and the charge collector layer are coexistence in a same paper substrate, which was further encapsulated. The encapsulation layers have the function of protecting and prolonging the life of the device. The protective layers were made from normal paper or sponge paper. A copper tape has been used to connect the device with external circuit or measuring unit. **Figure 3.3(a)** shows the process of drawing electrode surface by pencil and **Figure 3.3(b)** and **3.3(c)** show the conductivity of the electrode using different grade of pencils (6B and 8B).

The lateral resistance of the 6B and 8B pencil drawn electrode were both measured with values of 1329 Ω and 500 Ω , respectively.

When a mechanical force is applied on the FPP, a deformation occurs in the molecular structure consequently there is a physical approximation of the polymeric chains. The localized deformation in the molecular networks results a raising of charge carrier density in that region, consequently the Fermi level (is the energy level which is occupied by the electron orbital at 0° K) pinning. This mechanism fundamentally promotes the charge transfer mechanism between that deformed area (is PPy network) and the nearest stable energy level (*i.e.* electrode).^[35] When the stress is released, the result will be an de-pinning of the Fermi level due to the scarcity of charge carriers at the surface and the charge transfer will stop. This localized electronic scarcity was originated due to the expansion of the PPy chains and the transferring of charge carriers after releasing the stress. But this scarcity of charge in the molecular network will soon be balanced by the charge diffusion from the adjacent affected areas with the higher charge concentration. This charge transportation mechanism took place through hopping mechanism.

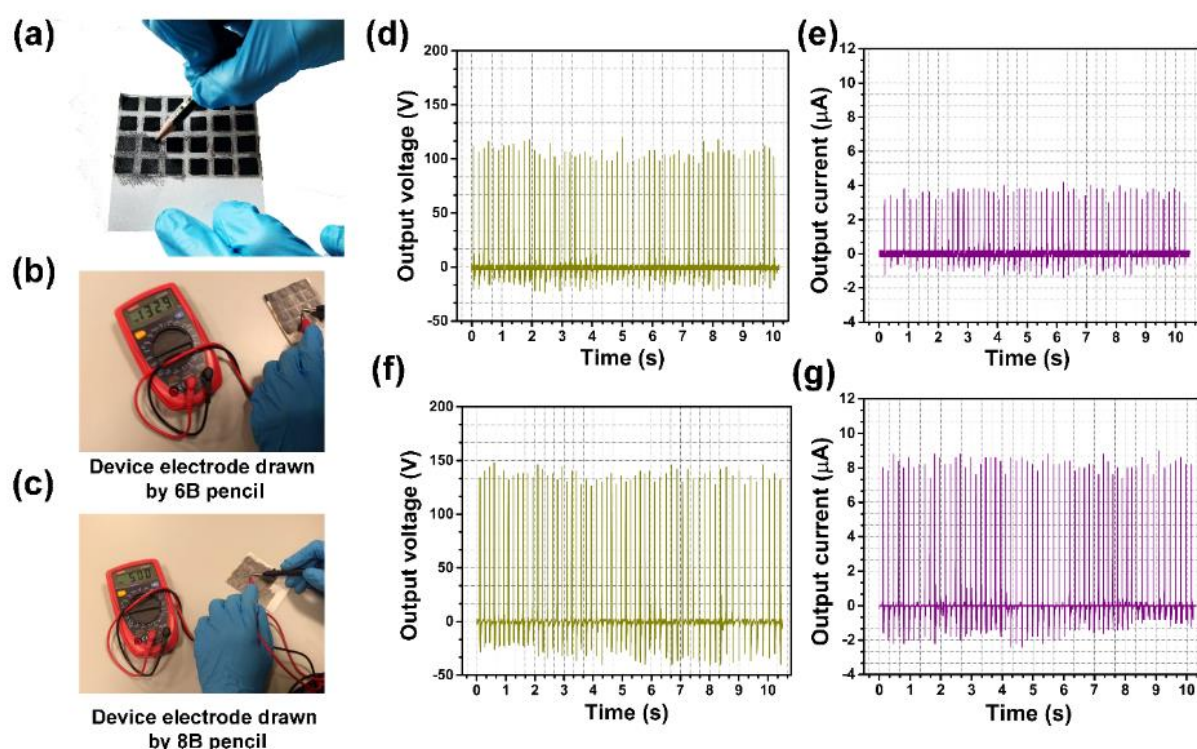


Figure 3.3: (a) Drawing the graphite pencil electrode directly on the FPP; (b), (c) Lateral resistance of 6B and 8B pencil electrode; (d),(e) Mechano-responsive output voltage and current, respectively, of 6B electrode device; (f),(g) Mechano-responsive output voltage and current, respectively, of 8B electrode device.

Figure 3.3 (d) - (g) show the output open circuit voltage (V_{oc}) and short circuit current (I_{sc}). The measurement data were obtained from an oscilloscope and customized electrical circuit. I_{sc} measurements were performed using 10 M Ω resistance and a 100 Ω resistance in series.

The output voltage of the device with 6B pencil electrode (D_{6BE}) obtained in range of 95-120 V and for the device with 8B pencil electrode (D_{8BE}), obtained in the range of 125-148 V, with the increment of 23%. The output current of device D_{6BE} and D_{8BE} is close to 3-4.2 μA , and 7.3-9 μA respectively, which represent a 114% increment. The change in electrical response is because of electrical nature of electrode

layer. It has been shown that resistance of electrode layer changes with the quality pencil grade *i.e.* the percentage of carbon present on pencil. An increase in carbon percentage would lead to a decrease in resistance and hence the improvement in electrical output from the device.

Output performance depending on the separation of the electrode

In a general theory, to get the electrical energy from triboelectric mechanism, a separation is required between two different layers that become close with mechanical force to each other. However, the above-mentioned device was designed without any physical separation between electrode and active materials. Here we have designed two device structure, integrated with silver screen printed electrode. One is without physical separation (D_{WSE}) and another is with separation (D_{SE}). **Figure 3.4** shows the schematic and real device structure for all three types.

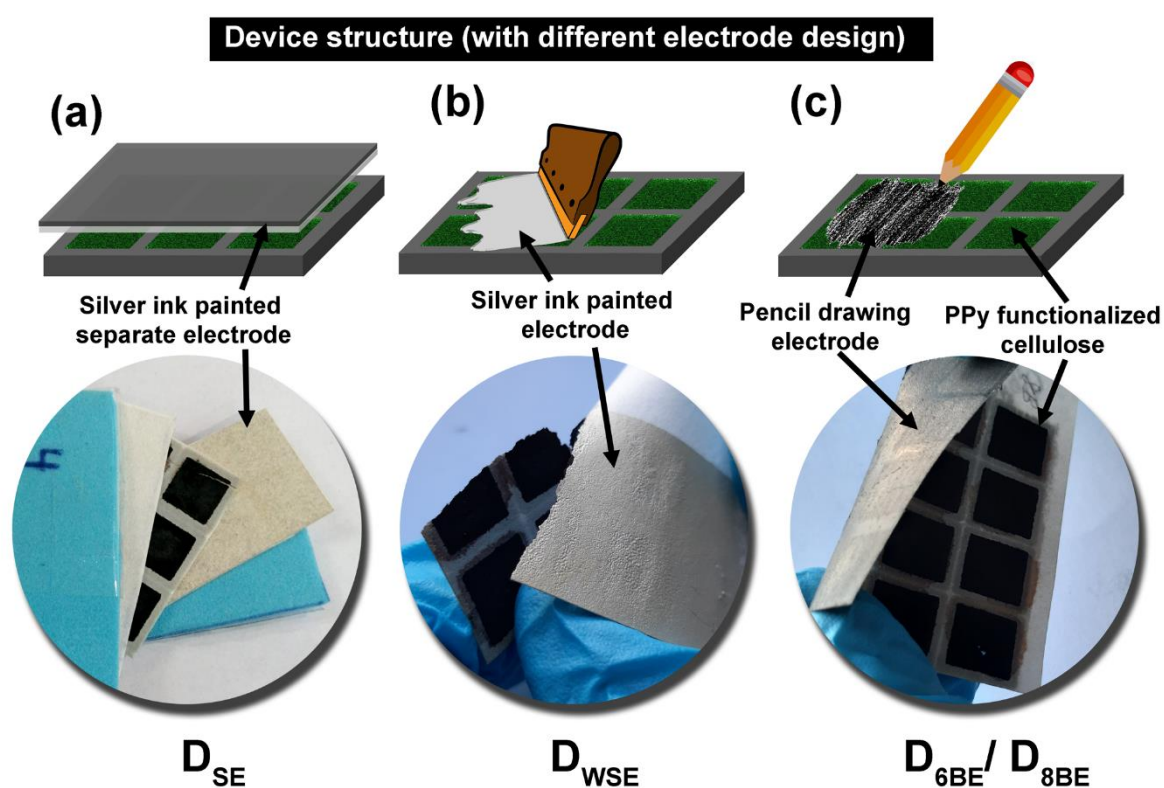


Figure 3.4: Schematic design of three different architectures of paper-based energy harvesting devices and their real images.

Here silver is used instead of graphite to investigate the influence of separation of electrode on mechanical energy harvesting system as well.

When at the electrode-polymer interface exist an increase of charge carriers that will result in Fermi-level pinning and a translocation of electrons to the electrode.

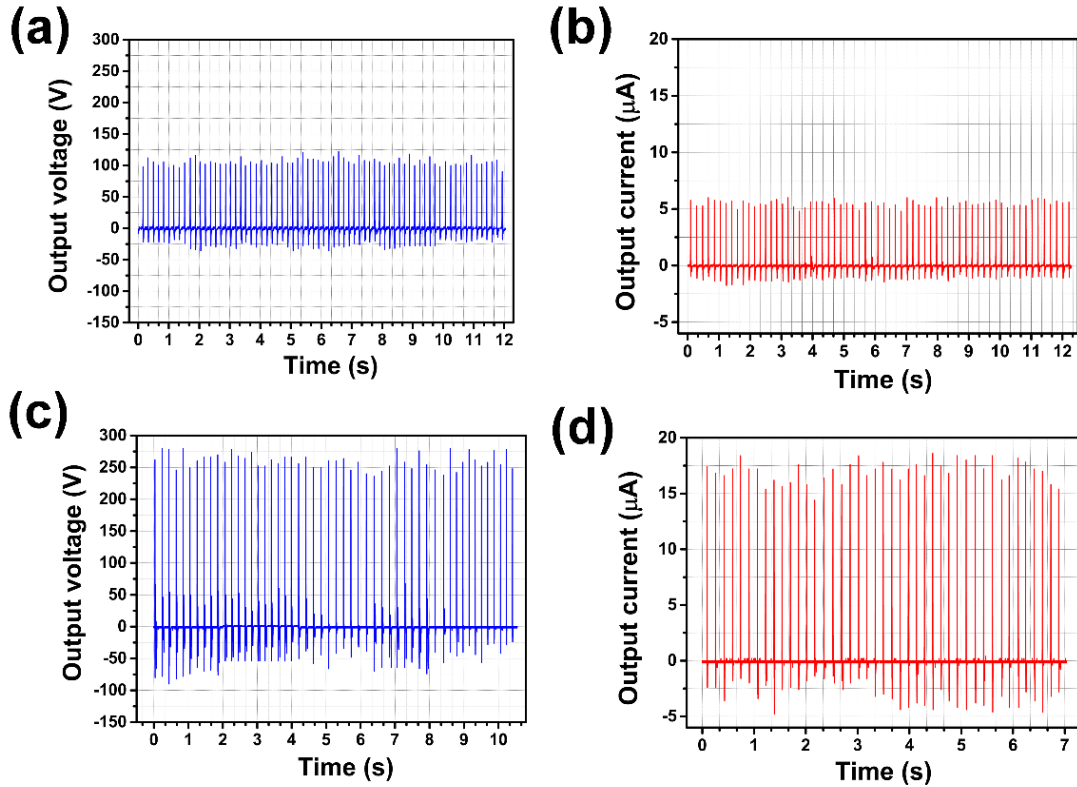


Figure 3.5: (a),(b) Mechano-responsive output voltage and current, respectively, of device with separation of electrode; (c)(d) Mechano-responsive output voltage and current, respectively, of device without separation of electrode.

Figure 3.5 (a) and (b) show the open-circuit output voltage (V_{oc}) and short circuit current (I_{sc}) in a range of values between 90-120 V and 4.8-5.5 μA respectively for the device D_{SE} . For the device without physical separation, D_{WSE} , the output voltage and current are in a range of values between 225-275 V and 15-18 μA respectively. It is clearly shown that the D_{WSE} exhibits 129% improvement in V_{oc} and 227% in I_{sc} . The same electrode material (silver ink) was used for both electrodes. The human hand was used for testing the device performed by tapping the device. The force applied and the frequency were maintained constant during both tests.

But why the D_{WSE} shows much more efficiency than D_{SE} ?

For device D_{WSE} , there is no physical separation between electrode and PPy/cellulose layer, that increases the effective surface contact area between them. But due to the micro roughness of paper surface with its porous structure, the PPy/cellulose composite act as a sponge that allows effective deformation (squeezing and spreading) while stress employ/release on the device. When a mechanical stress is applied, the deformation of the molecular structure into the polymer/cellulose composite will be initiating charge translocation mechanism between AL and CCL. So due to the co-existential layers (AL and CCL) the effective surface area increases much more compared to the device, D_{SE} , which is with physical separation, consequently, would improve the performance of the device.

All three types of device images with schematic diagram has been shown in **Figure 3.4**.

Output performance: power density and current density

By nature, electrical energy harvested from the device is an AC characteristic. In order to get a DC output, a full wave rectifier circuit needs to be added. To calculate the power density of the device, a series of resistors (values varied from 55 k Ω to 150 M Ω) were added to a rectifier circuit. The schematic of converter circuit has been shown in **Figure 3.6**. Using the average output voltage associated to each different load of resistance, it is possible to calculate the power density from the equation $P = I^2 \times R$.

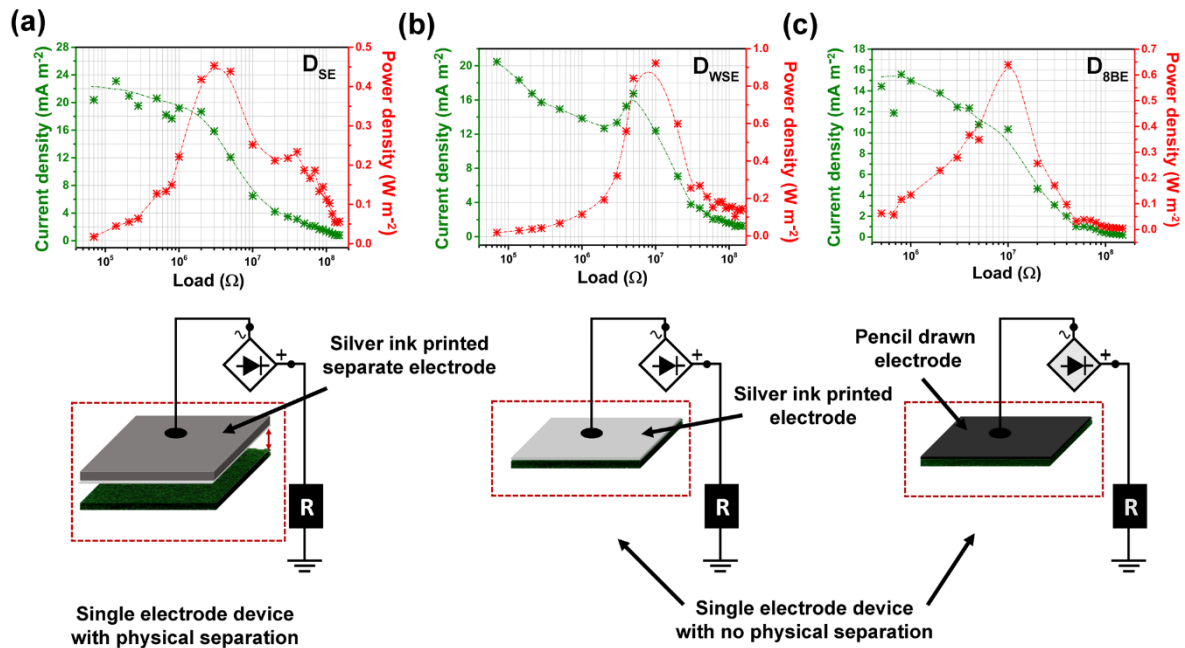


Figure 3.6: Results obtained for the current density and power density curves and schematic of rectifier circuit: (a) Paper-based device with separated silver electrode; (b) Paper-based device without separated silver electrode; (c) (b) Paper-based device without.

Table 1 indicates the comparison results of electrical responses for three different devices D_{SE} , D_{WSE} and D_{8BE} . The maximum power density (P_{max}) was achieved by the device D_{WSE} ($P_{max}=0.91$ W m⁻²). This device (D_{WSE}) also achieved the maximum V_{oc} and I_{sc} . It would be expected that it also reached the maximum value of current density (I_{max}). However, this value was reached by the device D_{SE} ($I_{max}=23$ mA m⁻²). **Figure 3.6 (a)-(c)** show the current and power density against the load from 55 k Ω to 150 M Ω for three different devices D_{SE} , D_{WSE} and D_{8BE} , respectively. The D_{WSE} is able to light 53 LEDs simultaneously see in Annex section **Figure A.5**.

Table 1: Electrical characterization results for the paper-based devices with different electrode material.

Device Name	Device Structure	Electrode Material	Average V_{oc} (V)	Average I_{sc} (μ A)	Maximum Power Density (W m ⁻²)	Maximum Current Density (mA m ⁻²)
D_{SE}	With separation	Silver ink	110	5	0.6	23
D_{WSE}	Without separation	Silver ink	250	15	0.91	21
D_{8BE}	Without separation	8B graphite pencil	135	8	0.65	15.7

3.3 Self-powered paper: Real-Field Applications

Human-interactive electronic barcode: Swipe test

In this thesis work, we have already analysed several electrical output characteristics for different types of device structures. We have already observed that the device with silver electrode and without separation (D_{WSE}) shows better efficiency and response among all three devices. So, for real-life application we used the design of D_{WSE} . It is already explained how the device generates electrical signal against any kind of human-interaction such as finger touch, slap, or swapping. From our previous experiment, it has been known that the electrical signal depends on the area of device. The bigger area generates much more intensity compare to the smaller surface area device. Therefore, using these characteristics, the idea of the electronic barcode is to architect device with unique arrays of bigger and small (the half of the bigger cell surface area) energy harvesting cells. The different combination of bigger and small energy harvesting cell can be identified with unique barcode which can generate high and low electrical signals, respectively while swapping. Furthermore, these high and low signals can be programmed as “1” and “0” binary codes. Several random electronic barcodes were created, consisting of bigger and smaller cells. The size of the smaller cell is $4.5 \times 22.5 \text{ mm}^2$ and for bigger cell it is $7.5 \times 22.5 \text{ mm}^2$. Each line was functionalized through *in-situ* polymerization following the same optimized method as discussed in materials and methods section. The rest of the process proceeded in the same way as energy harvesting devices.

Figure 3.7 shows the different design of electronic barcodes. The frontside of the device which is constituted by the Active layer (AL) and the backside were the electrodes that are directly printed by the silver ink paint and graphite pencil.

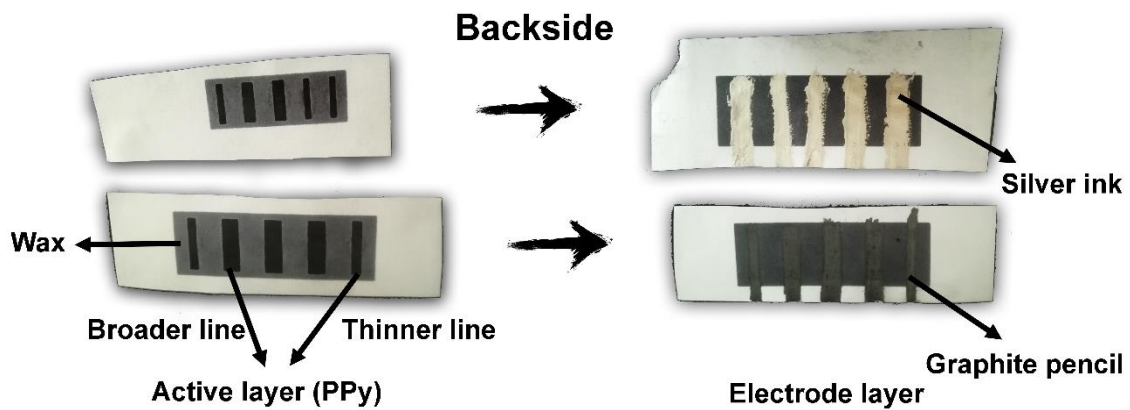


Figure 3.7: Schematic of frontside and backside of a Tag device used for security systems. Consisting of broader lines and thinner lines and without separating the electrode with the AL.

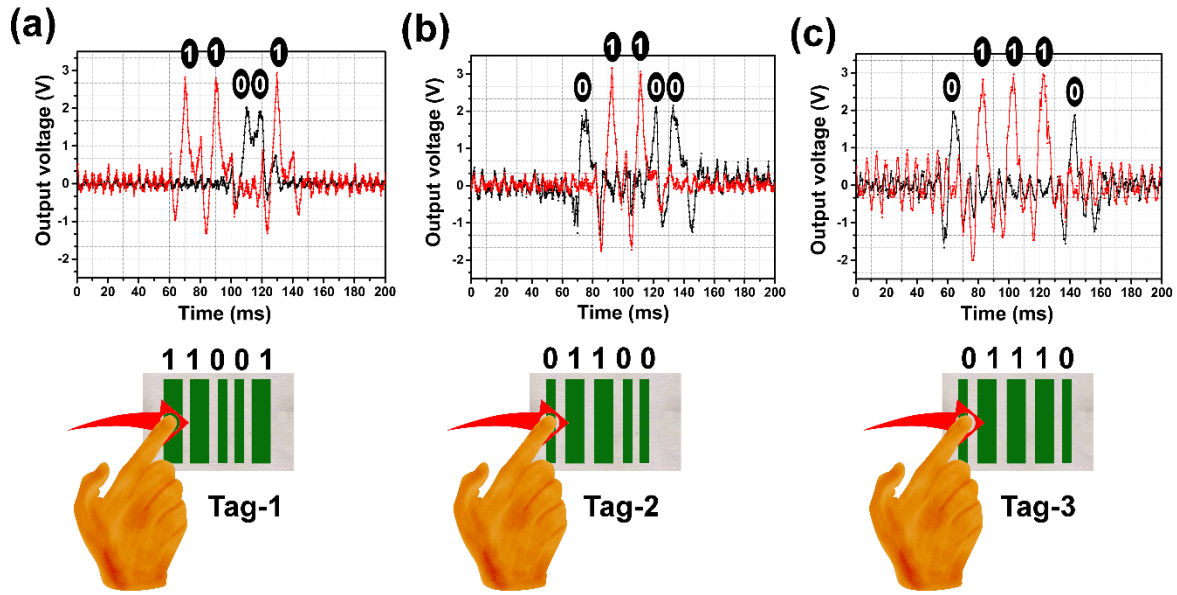


Figure 3.8: Swipe test that is performed in less than one second with a finger to slide over the tag: (a), (b), (c) The results obtained are the V_{oc} . It is possible to observe that the broader lines have an output voltage of about 3V and for the thinner lines 2V. The voltage can be classified in a binary system, with 1 being the highest and 0 the lowest.

In order to study the influence of the mechanical stimuli in the different size lines, the V_{oc} measurements were performed by recurring to a standard oscilloscope, where the smaller cells were connected to channel 1 and the bigger cells were connected to channel 2 of the oscilloscope. (see in Annex section **Figure A.4**).

On average, each test is performed at a swiping speed of 95 mm/s and the force of a male human hand (70 kg weight, 190 cm height) scrolling on the phone.

It is easy to conclude that different areas of Active Layer will give different output voltages. A higher contact area will result in more localized pressure zones, consequently the charge transfer mechanism will be initiated in these areas, promoting a larger amount of charge carriers translocating from AL to the electrode. In average, the smaller cells have an output voltage of 2V, and the bigger cells have an output voltage of 3V.

This technology can be used on a self-powered security system. The output voltage will be read by the Arduino which will classify the high and low voltages as “1”, “0” in binary system. This information will be sent by wireless communication. Depending on the different combination of output signal such as “1-1-0-0-1”, “0-1-1-0-0” or “0-1-1-1-0” can be defined as different information and can be stored in a memory. When we swipe the correct code, the information will appear to authenticate products. This electronic tag can easily be connected through mobile or PC.

Figure 3.9 shows the schematic illustration of the future application of the electronic tag.



Figure 3.9: An illustration of future application of self-powered electronic tag, which can be embedded in personal ID card or packaging. The particular arrays of device will generate particular electrical signal, which can be converted as binary code and transmitted through wireless and communicate with the security system such as “Door Open”, or “Product Authentication”

Touch-interactive R-G-B coding via wireless communication

For the applications, our paper-based energy harvester can scavenge different kinds of human motion energies. This energy harvesting system is characterized by lower power and higher output voltage, which is enough to power some LEDs when a person keeps tapping the device. However, to power more complex electronic equipment, it is necessary to use capacitors. Capacitor will store electrical energy when the device has an AC characteristic and for that will connect the device to a bridge rectifier. The storage energy will power the equipment.

Going beyond an energy harvesting system is one of the focus in this thesis, using the paper-based devices in real-fields applications. The electronic part implanted to our devices is based on a platform ESP32 or Arduino Uno. This platform was used to read the analog input signals from the self-powered touch-interactive paper and convert them to digital signal, in order to use these applications in connected appliances, wireless inventory trackers, etc. To use these devices in Internet of things (IoT) an ESP32 was used. ESP32 is a platform similar to Arduino Uno with integrated Wi-Fi and dual-mode Bluetooth. We used the ESP32 hardware to setup an HTTP for communication. The microcontroller ESP32 creates

its own Asynchronous Web server, where other devices can connect by using right password. It is possible to define the Wi-Fi server name and password. (For example, **SSID:** “Clean” and **Password:** “ENERGY”). To write the code to program the Arduino Uno and ESP we used the Arduino IDE software. Some ESP32 modules do not upload the sketches automatically, giving out the following error: “Failed to connect to ESP32: Timed out waiting for packet header”. To rectify this error a 10 μ F capacitor with positive (+) side connected to the Enable pin (EN,GPIO9) and negative(-) side attached to the board’s ground.ESP32 can send several sensor readings to the Asynchronous Web Server without the need to read them directly.

The R-G-B device use three touch-interactive energy harvester devices connected to an Arduino. Each device represents a color on R-G-B color model. The name of the model comes from the initials of the three primary colors, red, green, and blue.

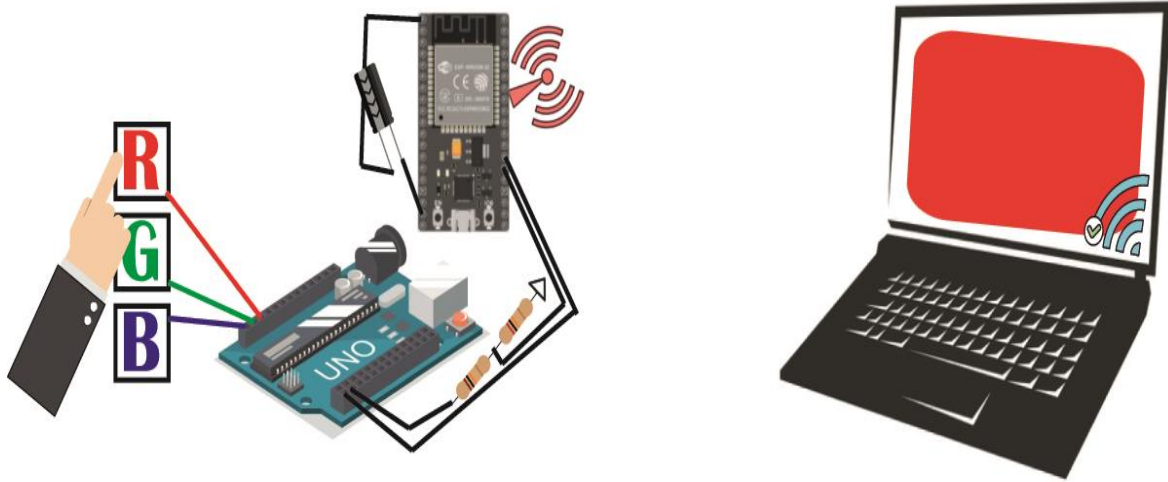


***Figure 3.10:** Schematic of "RGB device": Showing three touch-interactive energy harvester devices connected to an Arduino. When one or more devices are pressed, and the Arduino will receive this input and will return the associated color or colors. This output will be sent via the ESP32 microcontroller, which has Wi-Fi. A computer connected to a Wi-Fi network will receive the information and show the color. In this particular case, the example for the red color is shown.*

The principle of operation of our R-G-B application is to press one or more of the touch-interactive devices. Each device is attached to its own board pin. When we tap a touch-interactive device each sensor reading will be associated to a particular pin. The reads from each pin will be either binary 1 (if voltage reading > 100, which results from tapping) or binary 0 (if voltage reading < 100, which results from tapping). The comparative value is 100 and not 0 in order to account for value noise. One binary value is associated to a variable which is associated to each pins GPIO. Then, the ESP32 will send these values to the server which is accessible by using a particular link. With Python software we access the link, get the binary values and translate them to the chosen output. For example, if RED touch-interactive device is pressed, the color red will appear on computer. If the RED and BLUE touch-interactive devices are pressed the output will be magenta. (See **Annex 3**)

It is possible to connect more inputs and increase the complexity of the application. However, the ESP32 cannot use more than 4 pins to convert analog to digital while having the Wi-Fi network online. To deal

with the problem of having more than 4 inputs can be used an Arduino Uno to read and convert some of the inputs and establishing an UART (Universal Asynchronous Receiver-Transmitter) connection with the ESP32. The ESP32 and Arduino will be transmitting data to one another directly through a wire.

A Real-time video (SV2) of operating mode of the R-G-B device can be watched at <https://drive.google.com/file/d/1E8hIH0qcUGAiARH9tIAxnBQLHhz09KGM/view?usp=sharing>

3.4 Green device: A proof of biodegradability

To check the extent of environment friendly behavior of our manufactured device, we have burnt the device completely and did the analytical measurement by Raman. **Figure 3.11** shows the snap shots during the burning process. It can be seen that the device completely burns and form a black residual. To check the elemental analysis, we did Raman spectroscopy of the residuals part. Here we examined by adopting two process. (i) Device was burn for short time and (ii) device was burnt for long time. In both the cases, Raman shows the peak which corresponds to carbon. The main features in the Raman spectra of carbon materials are the G band (the graphitic band) and the D band (the disorder band). It is possible to see the graphite lattice (G band) at 1579 cm^{-1} as well as the disorder band caused by the graphite edges (D band) at approximately 1354 cm^{-1} . Only the long time burn device shows a high sharp peak intensity that indicates the high crystalline phase of carbon. It is confirmed that our device does not produce any toxic residuals after burning and produce only carbon.

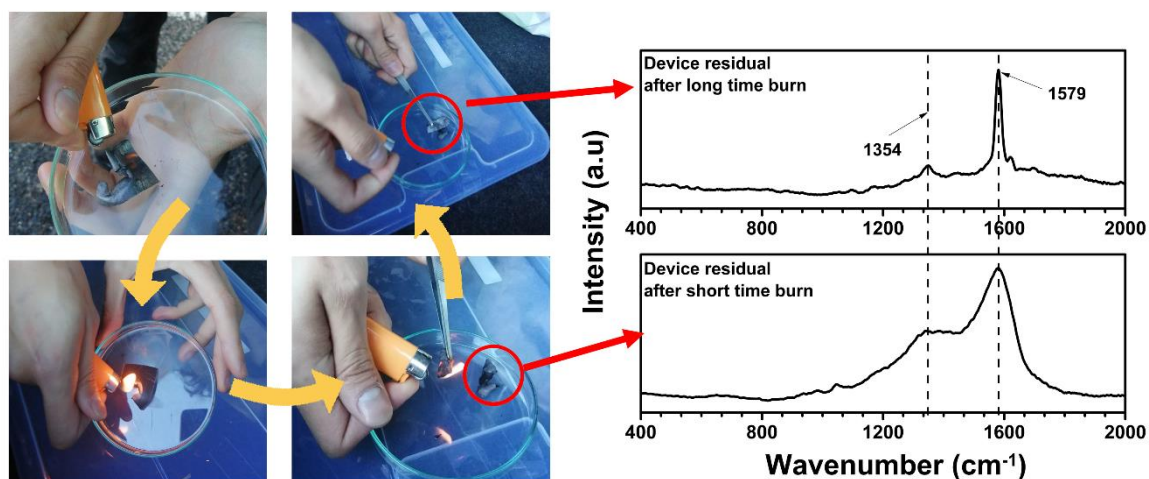


Figure 3.11: Snap shots of the device burning process. Raman spectroscopy analysis of black residuals that has been achieved after burning the device.

4. Conclusions and Future Perspectives

This work studies a new concept of energy harvesting system taking into account two very important premises: clean energy harvesting and zero e-waste. Paper has been used as the key material for manufacturing the device because of its flexible, low cost and biodegradable nature. Furthermore, graphite pencil was used in some of the devices for electrode layer, which makes one step ahead to bring the technology low-cost and green. The vision of the thesis work is to support and promote the agenda of United Nation 2030 sustainable goals and European Union green deal. The paper-based device that has been designed and developed during this thesis program, will work under any kind of human-interaction and generates electrical energy. Further, these human-interactive electrical signal has also been communicated through wireless system for next generation applications in self-powered security system. Though the challenging part during this work progress was to stably functionalize the paper substrates and apply it in real-life application. As a prototyped application, we have designed the electronic tag for security purpose.

In order to apply the simple pristine paper in such electronic application, it had to be functionalized with polypyrrole (PPy), since paper itself has no capacity for charge generating. After the functionalization of paper with PPy through *in-situ* polymerization technique, PPy/cellulose composite paper substrate showed a very good conductivity around 0.14 S m^{-1} . And further this paper shows the intrinsic properties of mechano-responsive charge transfer mechanism, which can produce electrical energy from kind of physical interaction.

In this work, we have designed single electrode energy harvesting systems, but the building block of the device was two different type: (i) electrode designed with a physical separation with the functionalized paper and (ii) the electrode directly fabricates on the functionalized paper, i.e there is no such a physical separation. These different structures enabled a significant improvement in the electrical functionality of the device. The device without separation of electrode has a V_{oc} of 250 V in average, which represents significant increase of 227% when compared with the device with separation, using silver ink as an electrode material.

Very interestingly, in this work graphite pencil has been used to simply draw the electrode on the paper projecting low-cost and green synthesis. For the graphite electrodes, as expected, the device with 8B pencil electrode showed a better electrical behavior regarding electrode with 6B pencil graphite. Most likely due to the fact that the different percentages of carbon present in the different pencils. And the results obtained exceeded expectations with maximum power density of 0.65 W m^{-2} and maximum current density of 15.7 mA m^{-2} .

The maximum power density of 0.91 W m^{-2} was achieved for the device without separation. The maximum current density was achieved by the device with separation 23 mA m^{-2} .

With this technology, the paper device has been used to lighting up to 53 LEDs instantaneously. However, the main goal was to design self-powered security system with this functionalized paper. We have initially designed an electronic tag, that can be used for identification of any objects. With simple swiping on the electronic tag, a unique code is generated that can be modified with a unique design of tag. Also, during this project wireless communication system has been built up, that are used to communicate electrical signals that are generated from the device. We have successfully, programmed a R-G-B coding system with our device. A colour mixing has been shown which can be further utilized to any security system.

The chemical and electrical properties of Polyaniline have been studied for a long time by our working group, while for Polypyrrole has been developed first time in this thesis work. Therefore, it required a optimization process to achieve standard, stable and high-efficiency functionalization. In some electrical tests, this polymer already stands out from PANI and it is expected that by continuing to study this polymer by doping-dedoping tuning, its electrical performance will be substantially superior. Also, different kind of conjugated polymers, such as PEDOT:PSS, P3HT can be investigated.

For how the device is really bio-degradable we burnt the device and did the analytical test of the ashes from the burnt device. The bio-degradability test was very promising, resulting in solid waste composed of carbon and does not produce any toxic solid residuals.

In order to further improve the device performance as well reduce ecological footprint, several aspects should be considered for future works.

To improve the focus toward environmentally sustainable research, it is important to use also recycled paper and study the impact that on Polymer/cellulose composite layer. It is important to get a good stability and resistance to mechanical force without compromising the electrical performance.

This technology has a lot of potential to grow in the electronic applications area. Humidity sensors, since Polypyrrole is very affected by humidity, further study can reveal the correlation between electrical properties and relative humidity. As we can conclude with this study that Polypyrrole is very sensitive to small mechanical stimuli, it would be interesting to study more deeply the variation of the electrical output with the applied force, and it could be applied to a force sensor. For the Tags used for the security system, instead of changing the surface area, it is possible to change the APS/Pyrrrole ratio and test the output performance. With that analyses it will be possible to vary the V_{oc} with the same force applied and the same surface area.

The concept can also be used in several applications. With the increase in the complexity of the applications, the number of electronic components necessary for the operation of the applications also increases. So, it is also necessary to work on the miniaturization of the electronic part and power management circuit.

5. References

- [1] T. A. Plan *et al.*, “Circular Economy Action Plan,” 2015.
- [2] C. P. Balde, V. Forti, V. Gray, R. Kuehr, and P. Stegmann, *The global e-waste monitor 2017: quantities, flows and resources*. United Nations University, International Telecommunication Union, no. December. 2017.
- [3] V. Forti, C. P. Balde, R. Kuehr, and G. Bel, *The Global E-waste Monitor 2020: Quantities, Flows, and the Circular Economy Potential*. 2020.
- [4] European Commission, “An ambitious EU circular economy package [Fact sheet],” *Commun. from Comm. to Eur. Parliam. Counc. Eur. Econ. Soc. Comm. Committe Reg.*, p. 2, 2015, [Online]. Available: https://ec.europa.eu/commission/sites/beta-political/files/circular-economy-factsheet-general_en.pdf.
- [5] R. Martins *et al.*, “Papertronics: Multigate paper transistor for multifunction applications,” *Appl. Mater. Today*, vol. 12, pp. 402–414, 2018, doi: 10.1016/j.apmt.2018.07.002.
- [6] G. Ferreira, S. Goswami, S. Nandy, L. Pereira, R. Martins, and E. Fortunato, “Touch-Interactive Flexible Sustainable Energy Harvester and Self-Powered Smart Card,” *Adv. Funct. Mater.*, vol. 30, no. 5, pp. 1–9, 2020, doi: 10.1002/adfm.201908994.
- [7] K. Mao *et al.*, “Paper-based microfluidics for rapid diagnostics and drug delivery,” *J. Control. Release*, vol. 322, no. February, pp. 187–199, 2020, doi: 10.1016/j.jconrel.2020.03.010.
- [8] X. S. Zhang, M. Su, J. Brugger, and B. Kim, “Penciling a triboelectric nanogenerator on paper for autonomous power MEMS applications,” *Nano Energy*, vol. 33, no. January, pp. 393–401, 2017, doi: 10.1016/j.nanoen.2017.01.053.
- [9] S. Goswami *et al.*, “‘Electro-Typing’ on a Carbon-Nanoparticles-Filled Polymeric Film using Conducting Atomic Force Microscopy,” *Adv. Mater.*, vol. 29, no. 47, pp. 1–9, 2017, doi: 10.1002/adma.201703079.
- [10] Y. Yin, K. Feng, C. Liu, and S. Fan, “A polymer supercapacitor capable of self-charging under light illumination,” *J. Phys. Chem. C*, vol. 119, no. 16, pp. 8488–8491, 2015, doi: 10.1021/acs.jpcc.5b00655.
- [11] C. Sekine, Y. Tsubata, T. Yamada, M. Kitano, and S. Doi, “Recent progress of high performance polymer OLED and OPV materials for organic printed electronics,” *Sci. Technol. Adv. Mater.*, vol. 15, no. 3, 2014, doi: 10.1088/1468-6996/15/3/034203.
- [12] T. R. Pavase *et al.*, *Recent advances of conjugated polymer (CP) nanocomposite-based chemical sensors and their applications in food spoilage detection: A comprehensive review*, vol. 273. Elsevier B.V., 2018.
- [13] S. Cete, M. Ozyurt, E. Yildirim, and D. Akin, “A novel biosensor with the use of polypyrrole–poly(sodium-4-styrenesulphonate) as a dopant in the determination of glucose,” *Chem. Pap.*, vol. 74, no. 3, pp. 799–808, 2020, doi: 10.1007/s11696-019-00907-6.
- [14] A. Guiseppi-Elie, “Electroconductive hydrogels: Synthesis, characterization and biomedical applications,” *Biomaterials*, vol. 31, no. 10, pp. 2701–2716, 2010, doi: 10.1016/j.biomaterials.2009.12.052.
- [15] B. Massoumi and A. A. Entezami, “Electrochemically stimulated 2-ethylhexyl phosphate (EHP) release through redox switching of conducting polypyrrole film and polypyrrole/poly (N-methylpyrrole) or self-doped polyaniline bilayers,” *Polym. Int.*, vol. 51, no. 6, pp. 555–560, 2002, doi: 10.1002/pi.885.
- [16] A. D. Bendrea, L. Cianga, and I. Cianga, *Review paper: Progress in the field of conducting polymers for tissue engineering applications*, vol. 26, no. 1. 2011.
- [17] L. Zhan *et al.*, “Coaxial Co₃O₄@polypyrrole core-shell nanowire arrays for high performance lithium ion batteries,” *Electrochim. Acta*, vol. 209, pp. 192–200, 2016, doi: 10.1016/j.electacta.2016.05.059.
- [18] Y. Wang, J. Duan, Y. Zhao, Z. Jiao, B. He, and Q. Tang, “Rain-responsive polypyrrole-graphene/PtCo electrodes for energy harvest,” *Electrochim. Acta*, vol. 285, pp. 139–148, 2018, doi: 10.1016/j.electacta.2018.07.210.
- [19] T. Sen, S. Mishra, and N. G. Shimpi, “Synthesis and sensing applications of polyaniline

- nanocomposites: A review,” *RSC Adv.*, vol. 6, no. 48, pp. 42196–42222, 2016, doi: 10.1039/c6ra03049a.
- [20] A. Afzal, F. A. Abuilaiwi, A. Habib, M. Awais, S. B. Waje, and M. A. Atieh, “Polypyrrole/carbon nanotube supercapacitors Technological advances and challenges,” *J. Power Sources*, vol. 352, pp. 174–186, 2017, doi: 10.1016/j.jpowsour.2017.03.128.
- [21] Z. Zhang, M. Liao, H. Lou, Y. Hu, X. Sun, and H. Peng, “Conjugated Polymers for Flexible Energy Harvesting and Storage,” *Adv. Mater.*, vol. 30, no. 13, pp. 1–19, 2018, doi: 10.1002/adma.201704261.
- [22] G. Ferreira, “Eco-energy Smart Card”: A human-interactive all paper based, mechanical energy harvester (Msc thesis), no. October. 2019.
- [23] V. K. Wong, J. H. Ho, and A. B. Chai, “Performance of a piezoelectric energy harvester in actual rain,” *Energy*, vol. 124, pp. 364–371, 2017, doi: 10.1016/j.energy.2017.02.015.
- [24] C. Covaci and A. Gontean, “Piezoelectric energy harvesting solutions: A review,” *Sensors (Switzerland)*, vol. 20, no. 12, pp. 1–37, 2020, doi: 10.3390/s20123512.
- [25] V. Slabov, S. Kopyl, M. P. Soares dos Santos, and A. L. Kholkin, “Natural and Eco-Friendly Materials for Triboelectric Energy Harvesting,” *Nano-Micro Lett.*, vol. 12, no. 1, 2020, doi: 10.1007/s40820-020-0373-y.
- [26] Y. Wang, Y. Yang, and Z. L. Wang, “Triboelectric nanogenerators as flexible power sources,” *npj Flex. Electron.*, vol. 1, no. 1, pp. 1–9, 2017, doi: 10.1038/s41528-017-0007-8.
- [27] Z. Yang, S. Zhou, J. Zu, and D. Inman, “High-Performance Piezoelectric Energy Harvesters and Their Applications,” *Joule*, vol. 2, no. 4, pp. 642–697, 2018, doi: 10.1016/j.joule.2018.03.011.
- [28] X. Shi, S. Chen, H. Zhang, J. Jiang, Z. Ma, and S. Gong, “Portable Self-Charging Power System via Integration of a Flexible Paper-Based Triboelectric Nanogenerator and Supercapacitor,” *ACS Sustain. Chem. Eng.*, vol. 7, no. 22, pp. 18657–18666, 2019, doi: 10.1021/acssuschemeng.9b05129.
- [29] I. G. David, D. E. Popa, and M. Buleandra, “Pencil graphite electrodes: A versatile tool in electroanalysis,” *J. Anal. Methods Chem.*, vol. 2017, no. Cv, 2017, doi: 10.1155/2017/1905968.
- [30] A. Bhattacharya, A. De Das, S. N. Bhattacharya, and S. Das, “Transport properties of FeCl₃ -doped polypyrroles at different dopant concentrations,” *Journal Phys. Condens. Matter*, vol. 10499, 1994, doi: 10.1088/0953-8984/6/48/011.
- [31] O. N. Efimov and R. Chem, “Related content Polypyrrole : a conducting polymer ; its synthesis , properties and applications Polypyrrole : a conducting polymer ; its synthesis , properties and applications,” 1997.
- [32] J. Stejskal and M. Trchová, “Surfactants and amino acids in the control of nanotubular morphology of polypyrrole and their effect on the conductivity,” *Colloid Polym. Sci.*, vol. 298, no. 3, pp. 319–325, 2020, doi: 10.1007/s00396-020-04607-6.
- [33] A. K. Mishra, “Conducting Polymers: Concepts and Applications,” *J. At. Mol. Condens. Nano Phys.*, vol. 5, no. 2, pp. 159–193, 2018, doi: 10.26713/jamcnp.v5i2.842.
- [34] M. Trchová and J. Stejskal, “Resonance Raman Spectroscopy of Conducting Polypyrrole Nanotubes: Disordered Surface versus Ordered Body,” *J. Phys. Chem. A*, vol. 122, no. 48, pp. 9298–9306, 2018, doi: 10.1021/acs.jpca.8b09794.
- [35] S. Goswami *et al.*, “Human-motion interactive energy harvester based on polyaniline functionalized textile fibers following metal/polymer mechano-responsive charge transfer mechanism,” *Nano Energy*, vol. 60, no. January, pp. 794–801, 2019, doi: 10.1016/j.nanoen.2019.04.012.

Annexes

Annex 1. – Chemical and Morphology Analyses

A PPy/cellulose composite was synthesized, which worked as the active layer (AL). The WCP is highly porous and has lower fiber density which allows to form a cauliflower-like morphology by *in-situ* polymerization. **Figure A.1** shows a FESEM image of raw paper (WCP) without functionalization.

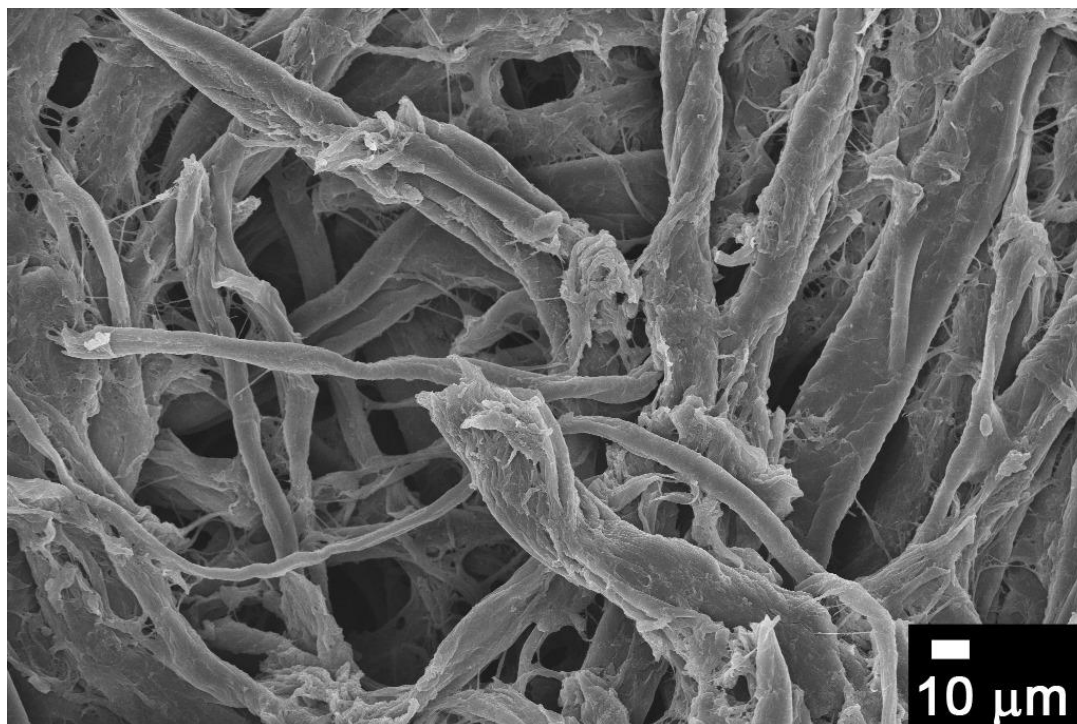


Figure A.1: FESEM image of raw Whatman Chromatography Paper.

The electrical properties of FPP were studied inside an humidity chamber in order to understand the effects of humidity in our devices. This chamber is connected to a humidity sensor, so that it is possible control the variation of humidity.

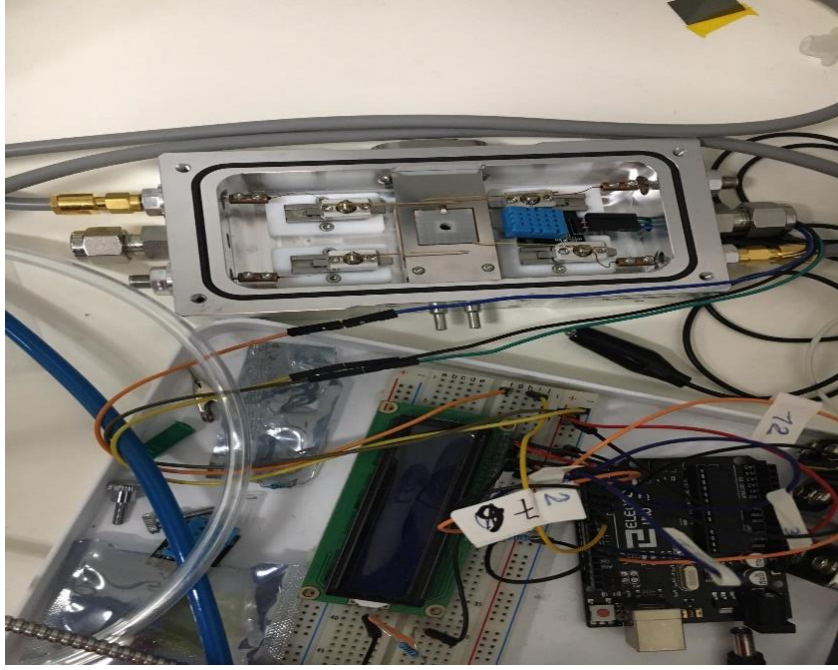


Figure A.2: Humidity sensor setup

3-hour tests were performed for different humidity values: 5%, 20%, 40% and 80%. It is possible to verify that for same device the different relative humidity affects the electrical performance.

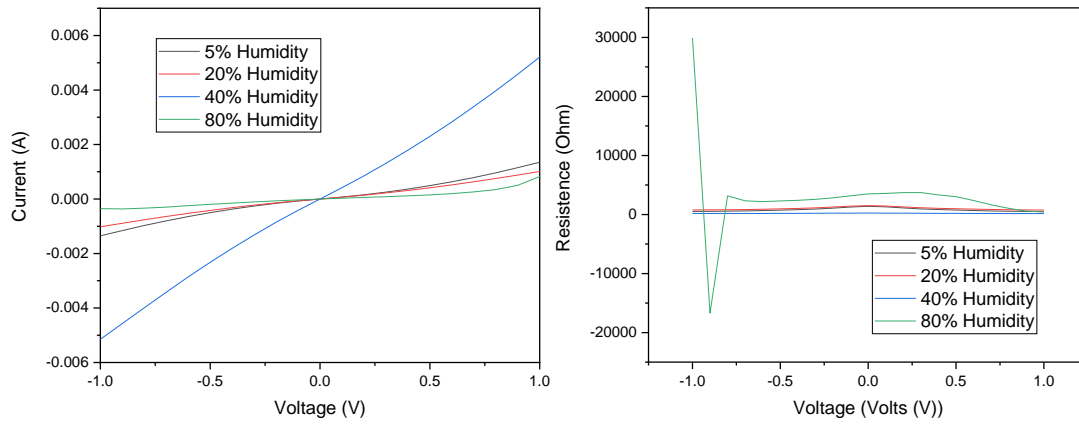


Figure A.3: a) I-V curves of the humidity sensor at different relative humidity. b) Graphic of device resistance at different relative humidity.

Annex 2. – Electrical Analyses

Since the oscilloscope has only 2 channels, it was necessary to connect the small cells in series to channel 1 and the large cells in series to channel 2. Thus, it is possible to read 5 signal inputs without having to have 5 channels available.

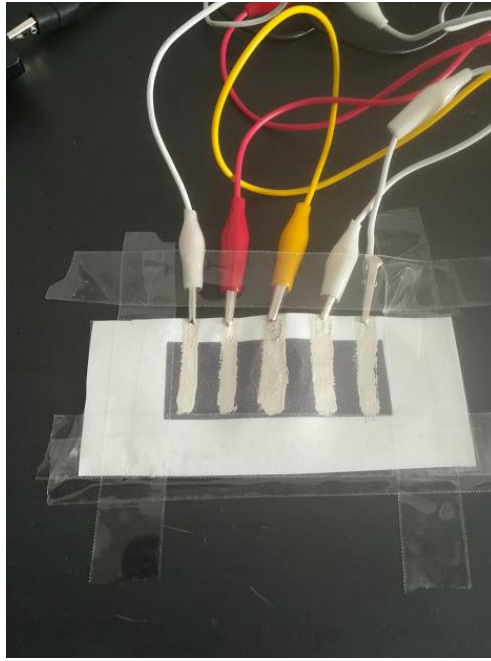


Figure A.4: Snapshot of the connections of each line of Tag device with oscilloscope.

The D_{WSE} is able to instantaneously light up to 53 LEDs.

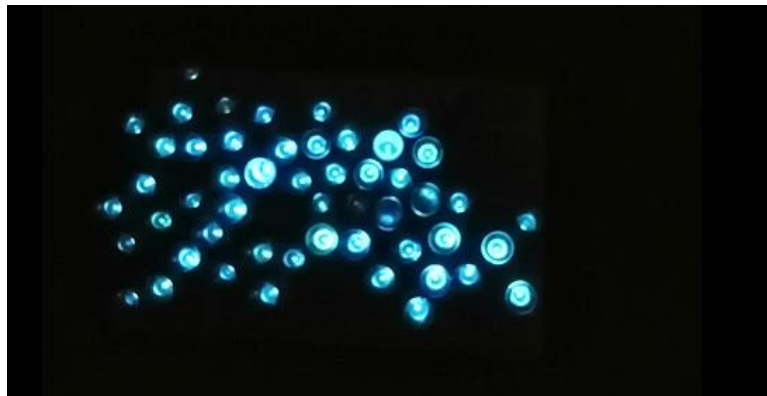


Figure A.5: Snapshot of 53 LEDs lighting up during performance tests.

SV1: Real- time video of powering 53 LEDs in series configuration with our energy harvesting device.

<https://drive.google.com/file/d/1XxmqqkGYP1yck3glkC91aSYIJoTTlk7Jd/view?usp=sharing>

Annex 3. – Self-powered paper Real- Field Application

The RGB color model is an additive color model. The mixing of the three additive primary colors will produce a broad array of colors.

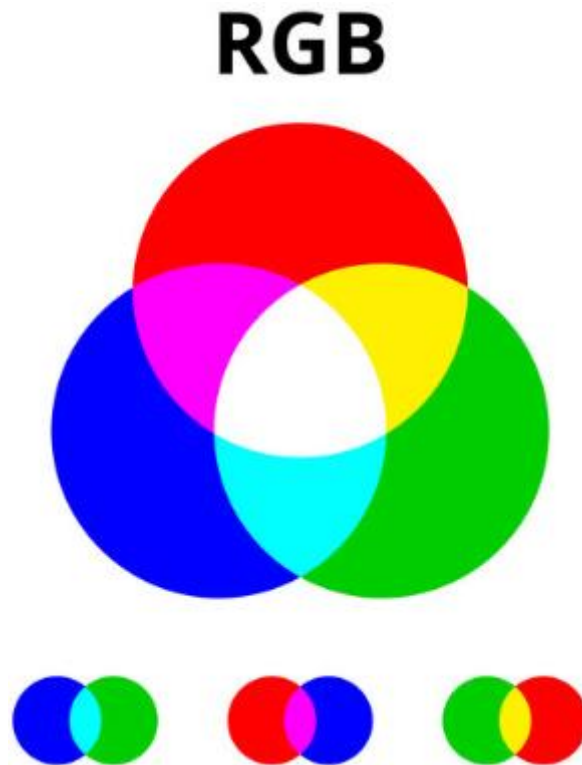


Figure A.6: RGB Color Codes Chart

Annex 4. – Self-powered PDMS device

During this thesis, some work was also done with PDMS. In order to disperse the polypyrrole in the PDMS, it was necessary to prepare PPy as a powder. The reagents used and their concentrations were the same used in the laboratory work developed in this thesis. However, instead of using the drop-cast technique, polypyrrole is synthesized in a beaker and then filtered and taken to the oven to retain water and a black powder is obtained. The chosen electrode to be used on this kind of devices was laser-printed graphene on Kapton due to their flexible nature.

To the fabrication of the device a layer of PDMS is spread over an area bounded over a silicon wafer. Kapton with graphite was added on top of the layer in contact with the PDMS which was then cured and peeled off. The device is presented on **Figure A.7**.

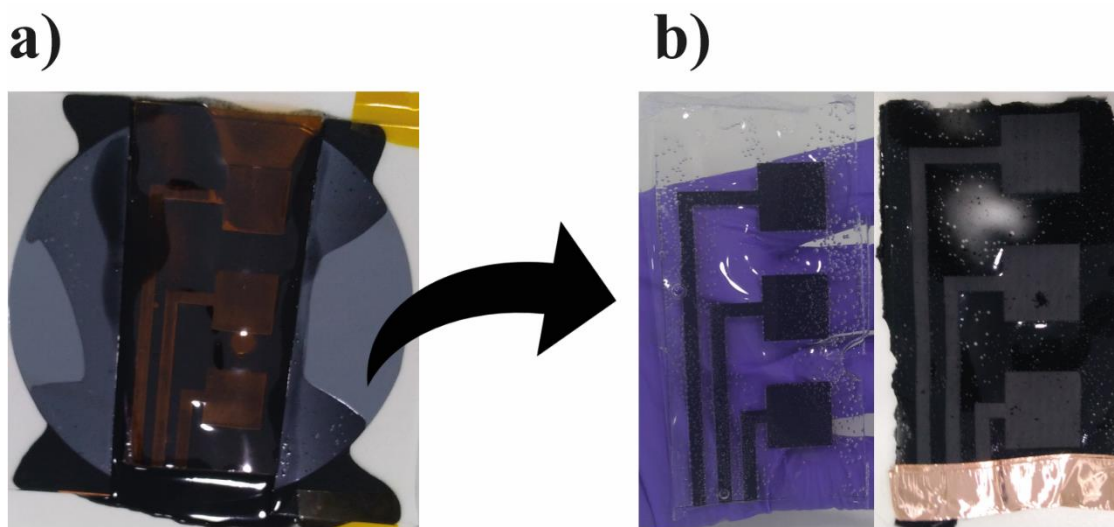


Figure A.7: a) The PDMS device before Kapton peeling off, b) PDMS devices without and with Polypyrrole after peeling off, respectively.

The results obtained are very promising with output voltage reaching the 160V and output current reaching 13 μ A. These devices can be integrated into numerous technologies.

Supporting Real-time video:

1. **Supporting Video SV1:** Real- time video of powering 53 LEDs in series configuration with our energy harvesting device.

<https://drive.google.com/file/d/1XxmQkGYP1yck3glkC91aSYlJoTTIk7Jd/view?usp=sharing>

2. **Supporting Video SV2:** Real-time video of operating mode of the R-G-B device

<https://drive.google.com/file/d/1E8hIH0qcUGAiARH9tIAxnBQLHhz09KGM/view?usp=sharing>